Lamming G, Kolokotroni J, Harrison T, Penfold TJ, Clegg W, Waddell PG, Probert MR, Houlton A.

Structural Diversity and Argentophilic Interactions in 1-D Silver-based Coordination Polymers.

***Crystal Growth and Design* 2017**

Structural Diversity and Argentophilic Interactions in 1-D Silver-based Coordination Polymers

Glenn Lamming, James Kolokotroni, Thomas Harrison, Thomas J. Penfold, William Clegg, ♯ Paul G. Waddell,♯ Michael R. Probert,♯ Andrew Houlton*

Chemical Nanoscience Laboratory, School of Chemistry, Newcastle University, Newcastle upon Tyne, NE1 7RU. ♯Crystallography Laboratory, School of Chemistry, Newcastle University, Newcastle upon Tyne, NE1 7RU

KEYWORDS Silver, 1D, coordination polymer, argentophilic

Abstract A series of new 1D coordination polymer materials, based on Ag(I)-N bond formation, has been synthesized and structurally characterized by single crystal X-ray diffraction. Reactions between the poly-monodentate ligands based on (1E,1'E')-N,N'-(-bis(1-pyridin-3-yl)methanimine and Ag(I) salts give products which feature simple coordination chains or metallacyclic- and tape-based structures. For the simple chains these are as either isolated units, or assembled in dimeric and tetrameric arrangements through inter-metallic, argentophilic interactions. However, crystal packing effects and solvent inclusion are found to readily disrupt this type of bonding. DFT calculations provide an assessment of the bond order and the influence of anion binding on these interactions.

Introduction

Coordination polymers[1-3] based on d10 Ag(I) ions exhibit diverse structure types due to the metal's ability to adopt a range of coordination numbers and geometries.[2, 4-8] This makes structure design and prediction challenging, a fact further compounded by the typically weak labile nature of the silver-ligand bond.[4, 6, 9] For example, for commonly-used pyridyl ligands this is of the order of an intermolecular hydrogen bond interaction.[4] Intermolecular bonding can also arise from metal…metal interactions which, though historically important in simple salts, have only relatively recently been acknowledged in molecular materials and studied in detail.[10] This, so-called, argentophilicity provides yet another interaction type that can influence the organization of these extended molecular systems in the condensed crystalline phase.

Despite the difficulties of structural predictability, Ag(I)-coordination polymers exhibit a range of interesting and useful properties. These include luminescence,[11-14] anticancer[15] and antimicrobial activity,[16-17] even catalysis,[18] and therefore such materials remain important to prepare and characterize.

Mindful of these issues we have begun to explore the preparation of Ag(I) coordination polymers with ligands based on (1E,1'E)-N,N'-bis(1-pyridin-3-yl)methanimine (L1-L3, Scheme 1).[19] This type of poly-monodentate ligand offers pairs of two distinct N-donor types, pyridyl and imine. The inherent conformational flexibility allows for a variety of metal-ligand bond vector orientations by simple rotations of the NPyridyl-C and NImino-CBridge bonds and, hence, different chain topology (Scheme 2). Silver coordination polymers of this ligand type have been reported as, for

example, with the one-dimensional catena-poly[[(nitrato-κ2O,O')silver(I)]-μ-N,N'-bis(3-pyridylmethylidene)benzene-1,4-diamine], 1a.[20] Interestingly, 1a features unsupported argentophilic interactions [Ag…Ag 3.1631(8) Å] that generate a double-chain arrangement in the crystal lattice. The authors also highlight the role of □□□ interactions between benzene rings in this structural motif.

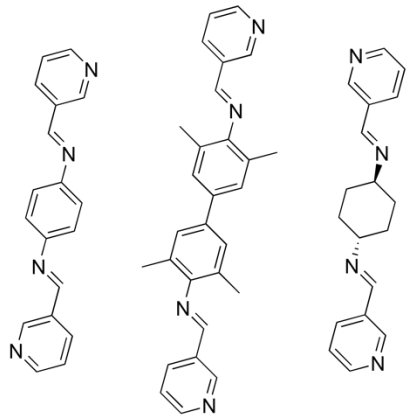

Scheme 1. (1E,1'E)-N,N'-(1,4-phenylene)bis(1-(pyridin-3-yl)methanimine) L1; (1E,1'E)-N,N'-(3,3',5,5'-tetramethyl-[1,1'-biphenyl]-4,4'-diyl)bis(1-(pyridin-3-yl)methanimine), L2; (1E,1'E)-N,N'-((1r,4r)-cyclohexane-1,4-diyl)bis(1-(pyridin-3-yl)methanimine), L3.

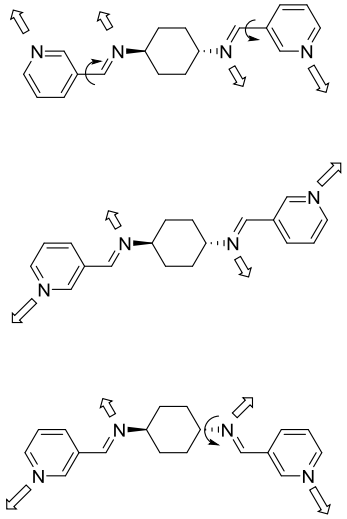

Scheme 2. Possible C–N and C–C bond rotations and the effect on the orientation of the metal–ligand bond vectors are illustrated for (top to bottom) syn-anti-syn, anti-anti-anti and anti-syn-anti conformers.

Here we report the structural characterization of new examples of one-dimensional silver-containing coordination polymers based on this general ligand type. In particular, we were interested in exploring the influence of the ligand framework on the resulting structures and the

propensity to form inter-chain argentophilic interactions. The three ligands, L1 - L3, differ in the nature of the central bridging group so as to consider aromatic vs. aliphatic effects (Scheme 1). Different counter anions were also explored with use of potentially coordinating (NO3-, Tosylate (Tos), trifluoroacetate (CF3CO2-), trifluoromethane sulfonate (TFM)) and non-coordinating (PF6-, BF4-) anions. Only materials that yielded crystalline products suitable for single crystal X-ray analysis are presented.

Discussion

Ligands L1-L3 were prepared in the E,E'-isomeric form using previously described methods.19 From a crystal growth viewpoint, the labile nature of typical Ag-N bonds allows formation of these polymeric materials at, or below, room temperature without the need for hydro- or solvo-thermal methods. We chose to perform the complexation reactions using a liquid/liquid diffusion method as recently reported by us.19 Solutions of dichloromethane containing the appropriate ligand (L1 – L3) and acetonitrile containing the silver salts were made up, individually cooled in cardice and then layered using a pipette. Products were typically isolated from 1:1 metal:ligand ratios, though some lack of stoichiometric control, quite common to the coordination chemistry of Ag(I) ions,8, 21 was apparent (vide infra). The reaction mixtures were stored in a freezer (-20oC) for 3 days before transfer to a refrigerator. This method typically provided samples suitable for single crystal X-ray analysis after 4-7 days. In some instances water present, or introduced deliberately, in the MeCN solvent was incorporated in the structures.

The crystal structure analyses reveal that eight of the ten metal complexes (2 – 5, 7 – 10) adopt the triclinic space group $P\bar{1}$, while compounds 1b and 6 crystallize in monoclinic P21/n and I2/a, respectively. All the compounds contain one-dimensional coordination polymers involving Ag–N bond formation at 2- or 3-coordinate Ag(I) centers. The details of the polymer chain structure and the extent of inter-chain interactions vary, however, with isolated single chains observed in 1b, 2 – 4 while argentophilically-associated dimer and tetramer arrangements are seen in 6, 9 and 8, respectively. Metallacyclic rings are found as either linked chains, in 5 and 10, or fused into a tape arrangement as in 7. A general feature is the preference for chain extension through coordinate bonding via pyridyl N-atoms. Only in two cases, 7 and 10, do the imino–N atoms also take part in metal-ion binding. Table 1 provides the crystallographic information for all the complexes 1b – 10 which are:

{[Ag(L1)NO3]}n, 1b

{[Ag(L1)]NO3·H2O}n 2

{[Ag(L1)(TFA)]}n, 3

{[Ag(L1)]PF6}n, 4

{[Ag(L1)1.5]BF4}n, 5

{[Ag(L2)]TFM}n, 6

{[Ag2(L3)(NO3)2]·2MeCN}n, 7

{[Ag(L3)(Tos)]·½H2O}n, 8

{[Ag(L3)(Tos)]·DCM}n, 9

{[Ag(L3)0.5(Tos)]·4H2O}n, 10

{[Ag(L1)NO3]}n, 1b

Reaction of L1 with AgNO3 yielded from separate experiments crystals identified as the previously reported 1a[20] and also a new polymorph 1b. Compound 1b crystallized in the monoclinic space group P21/n with the asymmetric unit comprising one unit each of Ag(I), L1 and NO3- and with all atoms in general positions. Compound 1b has a 1:1 Ag:ligand stoichiometry and contains a neutral "sine wave" polymeric chain based on distorted T-shape

Table 1. Crystallographic data for structures 1b – 10.

	1b	**2**	**3**	**4**	**5**	**6**	**7**	**8**	**9**	**10**
Empirical formula	C18H14AgN5O3	C18H16AgN5O4	C20H14AgF3N4O2	C18H14AgF6N4P	C27H21AgBF4N6	C29H26AgF3N4O3S	C22H26Ag2N8O6	C25H28AgN4O3.5S	C26H29AgCl2N4O3S	C16H25AgN2O7S
Formula weight	456.21	474.23	507.22	539.17	624.18	675.47	714.25	580.44	656.36	497.31
Temp /K	150	150	240	100	150	150	150	100	150	150
Crystal system	Monoclinic	Triclinic	Triclinic	Triclinic	Triclinic	Monoclinic	Triclinic	Triclinic	Triclinic	Triclinic
Space group	P21/n	P $\bar{1}$	P $\bar{1}$	P $\bar{1}$	P $\bar{1}$	I2/a	P $\bar{1}$	P $\bar{1}$	P $\bar{1}$	P $\bar{1}$
a/Å	5.1579(2)	4.9087(4)	4.72483(13)	5.2090(7)	8.7101(3)	17.5883(3)	8.0247(3)	12.586(4)	10.6683(7)	7.3262(2)
b/Å	15.9682(9)	8.8827(7)	9.5411(4)	8.4041(12)	10.2933(5)	10.51219(17)	8.1480(3)	12.603(4)	11.3914(8)	9.4198(3)
c/Å	21.0358(9)	10.7282(10)	21.7160(9)	11.0852(15)	14.5291(7)	34.0537(5)	10.6157(4)	18.483(7)	11.8059(7)	14.2104(4)
□/°	90	75.462(7)	89.427(4)	76.247(2)	85.739(4)	90	95.115(3)	70.605(3)	75.103(6)	89.965(2)
□/°	91.182(5)	84.917(7)	87.768(3)	89.323(3)	79.546(4)	103.1271(14)	95.458(3)	86.715(5)	75.633(6)	83.441(3)
□/°	90	76.056(7)	75.667(3)	75.087(3)	72.930(4)	90	109.856(4)	62.368(3)	81.974(6)	84.867(2)

	1b	**2**	**3**	**4**	**5**	**6**	**7**	**8**	**9**	**10**
Volume /Å3	1732.19(14)	439.26(7)	947.77(7)	454.86(11)	1224.26(10)	6131.69(17)	644.39(5)	2433.5(14)	1338.75(16)	970.31(5)
Z	4	1	2	1	2	8	1	4	2	2
□calc /gcm-1	1.749	1.793	1.777	1.968	1.693	1.463	1.841	1.584	1.628	1.702
□ /mm-1	9.607	1.185	1.118	1.179	7.141	6.379	12.663	0.881	1.067	9.708
F(000)	912.0	238.0	504.0	266.0	626.0	2736.0	356.0	11.88	668.0	508.0
Crystal size /mm3	0.29 × 0.12 × 0.04	0.25 × 0.2 × 0.11	0.39 × 0.07 × 0.05	0.052 × 0.048 × 0.011	0.19 × 0.05 × 0.03	0.26 × 0.14 × 0.11	0.24 × 0.07 × 0.03	0.40 × 0.06 × 0.03	0.2 × 0.09 × 0.08	0.37 × 0.25 × 0.17
Radiation	CuKα (λ = 1.54184)	MoKα (λ = 0.71073)	MoKα (λ = 0.71073)	Synchrotron (λ = 0.6899)	CuKα (λ = 1.54184)	CuKα (λ = 1.54184)	CuKα (λ = 1.54184)	Synchrotron(λ = 0.6889)	MoK□ (λ = 0.71073)	CuKα (λ = 1.54184)
2□ range for data collection /°	6.95 to 132.65	7.85 to 57.60	5.79 to 58.94	3.68 to 55.56	6.19 to 133.96	5.33 to 133.79	8.44 to 133.87	3.56 to 53.33	5.79 to 57.82	6.26 to 133.85
Index ranges	-6 ≤ h ≤ 4, -16 ≤ k ≤ 18, -22 ≤ l ≤ 24	-6 ≤ h ≤ 6, -11 ≤ k ≤ 11, -14 ≤ l ≤ 14	-6 ≤ h ≤ 6, -12 ≤ k ≤ 12, -28 ≤ l ≤ 29	-7 ≤ h ≤ 7, -11 ≤ k ≤ 11, -14 ≤ l ≤ 14	-6 ≤ h ≤ 10, -12 ≤ k ≤ 12, -17 ≤ l ≤ 17	-20 ≤ h ≤ 20, -11 ≤ k ≤ 12, -36 ≤ l ≤ 40	-9 ≤ h ≤ 9, -9 ≤ k ≤ 9, -12 ≤ l ≤ 12	-16 ≤ h ≤ 16, -16 ≤ k ≤ 16, -24 ≤ l ≤ 24	-14 ≤ h ≤ 13, -15 ≤ k ≤ 15, -15 ≤ l ≤ 15	-8 ≤ h ≤ 8, -10 ≤ k ≤ 11, -16 ≤ l ≤ 16
Reflections collected	7037	6999	30130	5624	17313	43887	9173	18793	22276	16941

	1b	**2**	**3**	**4**	**5**	**6**	**7**	**8**	**9**	**10**
Independent reflections	2782 [Rint = 0.0478, R□ = 0.0526]	2011 [Rint = 0.0493, R□ = 0.0575]	4537 [Rint = 0.0513, R□ = 0.0391]	2311 [Rint = 0.0497, R□ = 0.0563]	4334 [Rint = 0.0685, R□ = 0.0535]	5459 [Rint = 0.0416, R□ = 0.0209]	2279 [Rint = 0.0197, R□ = 0.0156]	18793 [Rint = 0.0150, R□ = 0.0501]	6194 [Rint = 0.0476, R□ = 0.0551]	3434 [Rint = 0.0529, R□ = 0.0311]
Data/restraints/parameters	2782/0/244	2011/107/151	4537/117/289	2311/0/139	4334/0/352	5459/175/392	2279/0/173	18793/3/632	6194/352/362	3434/32/269
Goodness-of-fit on F2	1.066	1.106	1.030	1.168	1.036	1.070	1.039	0.987	1.062	1.063
Final R indexes [I>2σ(I)]	R1 = 0.0498, wR2 = 0.1189	R1 = 0.0364, wR2 = 0.0613	R1 = 0.0480, wR2 = 0.1086	R1 = 0.0502, wR2 = 0.1384	R1 = 0.0337, wR2 = 0.0742	R1 = 0.0389, wR2 = 0.1011	R1 = 0.0152, wR2 = 0.0381	R1 = 0.0332, wR2 = 0.0846	R1 = 0.0508, wR2 = 0.1169	R1 = 0.0266, wR2 = 0.0672
Final R indexes [all data]	R1 = 0.0684, wR2 = 0.1271	R1 = 0.0458, wR2 = 0.0656	R1 = 0.0753, wR2 = 0.1218	R1 = 0.0506, wR2 = 0.1388	R1 = 0.0456, wR2 = 0.0808	R1 = 0.0454, wR2 = 0.1053	R1 = 0.0161, wR2 = 0.0385	R1 = 0.0387, wR2 = 0.0867	R1 = 0.0754, wR2 = 0.1319	R1 = 0.0273, wR2 = 0.0678
Largest diff. peak/hole / e Å-3	1.23/-0.58	0.41/-0.42	0.58/-0.57	3.62/-2.59	0.42/-0.51	0.88/-0.94	0.25/-0.30	0.92/-1.05	1.13/-1.29	0.77/-0.83

coordination geometry at Ag(I) (Figure 1). The polymer chain propagates along the crystallographic [$\bar{1}$02] direction with each adjacent unit generated by n-glide plane symmetry. Bond lengths to the metal ion are Ag1-N1 = 2.163(1) Å, Ag1-N4 2.154(1) Å and Ag-O1 = 2.527(1) Å with the angle N1-Ag-N4 = 155.5(1)o. The ligand adopts an anti-anti-anti conformation indicating a rotation around the C3Py–C7Im bond with metal binding as compared to solid-state structure(s) of L1 alone.22-23 The Ag…Ag distance is 17.917(3) Å along individual chains. The range of inter-planar angles between the three aromatic groups of individual L1 ligands is small, giving an essentially co-planar arrangement. This is also the case between adjacent ligands along the chain. There are no inter-chain Ag…Ag interactions and the shortest such distance is 5.15(1) Å.

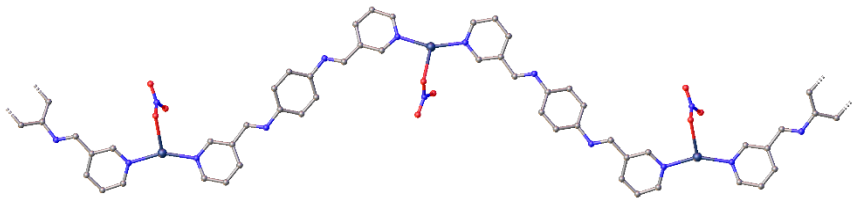

Figure 1. Structure of 1b showing a section of the neutral “sine wave” polymer chain.

By comparison, the polymorph 1a crystallizes in the triclinic space group P $\bar{1}$ and has been described20 as involving four-coordinate Ag(I) ions due to bidentate coordination by the NO3- anion. However, the Ag-O distances are long at >2.7 Å. The principal difference between the two polymorphs 1a and 1b is the presence of unsupported argentophilic bonding [Ag…Ag distance 3.163(1) Å] in the former. The Ag…Ag interactions form across an inversion center in a double-chain arrangement in which the aromatic groups are more eclipsed. The separation between these groups is rather long to be considered strong □□□ interactions [shortest centroid-centroid distance = 3.758 (3) Å between pyridyl rings]. A comparison of the difference between the positioning of neighboring chains in 1a and 1b is shown in Figure 2.

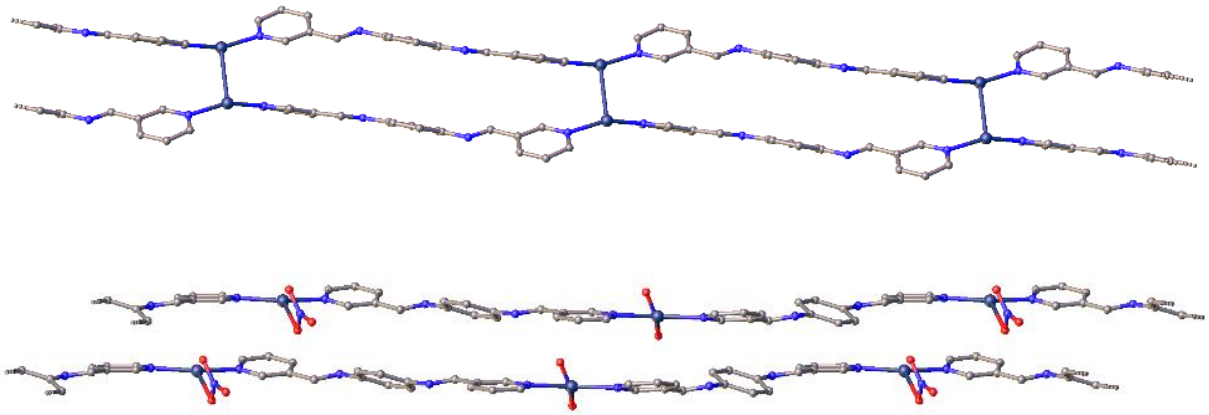

Figure 2. Views of adjacent chains in 1a (upper) and 1b (lower) chains highlighting the Ag…Ag pairing in the former and absence in the latter due to the "slipped" arrangement and lack of register between chains.

{[Ag(L1)]NO3·H2O}n 2

Compound 2, a hydrated solvomorph of 1, crystallizes in the triclinic space group P $\bar{1}$ with the asymmetric unit comprising half equivalents of Ag(I), L1, NO3 and a non-coordinated water molecule. The compound has a 1:1 Ag:ligand stoichiometry and contains a cationic polymer chain with a [1Ag + 1L] "saw-tooth" motif (Figure 3). The Ag(I) ion sits on an inversion center and the polymer chain is generated by inversion symmetry propagating in the [101] direction with strictly linear coordination. The unique Ag-N bond length is 2.165(1) Å. The ligand again adopts an anti-anti-anti conformation with the terminal pyridyl groups twisted out of the central phenyl plane by ~30.2o. The resulting Ag…Ag distance along individual chains is 18.110(1) Å. The nitrate anion and an occluded water molecule are disordered over two sites with the shortest Ag…O distances too long to be considered coordinating (Ag…OH2 2.738(1); NO3 2.807(1) Å).

Interestingly, despite what would appear to be an ideal arrangement of linear coordination geometry at the metal ion and co-planarity of the ligated pyridyl groups, there are no Ag…Ag interactions in the crystal structure. The shortest inter-metallic distance is 4.909(1) Å as neighboring chains are offset compared to 1a.

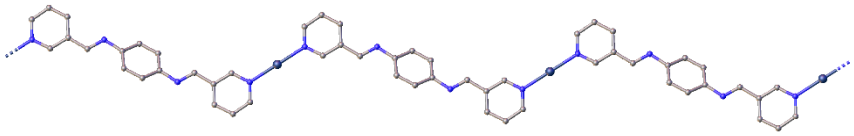

Figure 3. Section of a cationic polymeric chain in 2 highlighting the near co-planar {Py-Ag-Py} units and "saw-tooth" motif. The non-coordinated nitrate anion is omitted for clarity.

{[Ag(L1)(TFA)]}n 3

Substitution of the NO3- anion in 1b with trifluoroacetate gave 3 which crystallizes in the space group P $\bar{1}$, and the asymmetric unit is constituted by one unit each of Ag(I), and CF3CO2- and two crystallographically-independent half equivalents of L1. This 1:1 Ag:ligand stoichiometric compound forms [1Ag + 1L] neutral "sine wave" polymer chains, with each unit related to the next by inversion symmetry and propagating along the [104] direction (Figure 4). There is similarity to 1b with respects to the topology of the chains. The unique Ag(I) ion adopts a distorted T-shaped coordination geometry bonded by two, symmetry-equivalent, pyridyl N-atoms with the third site occupied by a monodentate CF3CO2- anion. The anion is rotationally disordered over three sites. Bond lengths to the metal ion are Ag1-N1 = 2.176(1) Å and Ag-OAvg = 2.417(1) Å with the angle N1-Ag-N1 = 155.3(1)o. Two independent L1 ligands lie across inversion centers and adopt an anti-anti-anti conformation and the two Ag…Ag distances generated along individual chains are essentially identical at 17.858(1) and 17.857(1) Å. As in 1b, the chains show no

metal…metal interactions in the crystal lattice with the shortest Ag…Ag distance being 4.725(1) Å. In 3 adjacent chains lie more directly above/below one another but are out of register w.r.t. the Ag(I) ion positions, a factor that may be attributable to the coordinating anion.

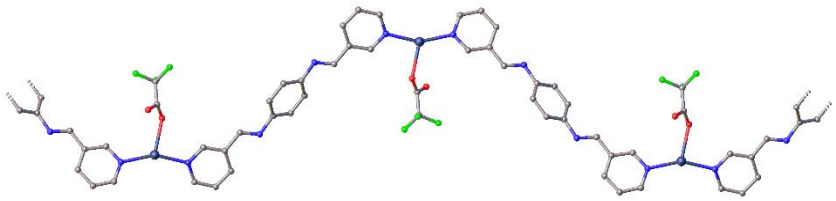

Figure 4. Molecular structure of 3 highlighting the one-dimensional "sine-wave" motif of the neutral coordination polymer chain.

{[Ag(L1)]PF6}n 4

Substitution of the trifluoroacetate by the non-coordinating PF6- anion gives compound 4. This crystallizes in the space group P $\bar{1}$, with the asymmetric unit bearing half equivalents of Ag(I), L1, and non-coordinating PF6- giving a 1:1 Ag:ligand stoichiometry. Both Ag(I) and P atoms sit in special positions with the resulting cationic polymer chain, generated by inversion symmetry, having a [1Ag +1L] "saw-tooth" topology similar to 2 (Figure 5). The Ag(I) ion sits on an inversion center with strictly linear coordination and a Ag-N bond length of 2.109(1) Å. The ligand again adopts an anti-anti-anti conformation with the terminal pyridyl groups twisted out of the central phenylene plane by 24.5(1)o. The Ag…Ag distances are 18.164(1) Å along individual chains while the shortest inter-chain distance at 5.209(1) Å is too long for metallophilic interaction.

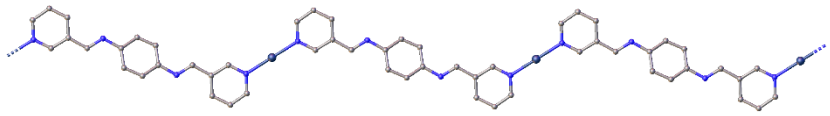

Figure 5. Molecular structure of a neutral coordination polymer chain in 4 highlighting the one-dimensional "saw-tooth" motif. The non-coordinated anion is omitted for clarity.

{[Ag(L1)1.5]BF4}n 5

With the non-coordinating BF4- anion compound 5 was obtained which again crystallized in the space group P $\bar{1}$. The asymmetric unit is constituted by one equivalent of Ag(I) and BF4- and three half units of L1 and all the atoms are in general positions. This resulting 1:1.5 Ag:ligand stoichiometric compound contains a cationic polymer comprising chains of metallacycles each half of which is related to the other by inversion symmetry (Figure 6). The unique Ag(I) ion is three-coordinate and the coordination comprises three Npyridyl donors. The Ag-N bonds are slightly longer than in the examples bearing two pyridyl donors, at Ag-N1 2.329(1) Å and Ag-N4 2.302(1) Å. This indicates some steric congestion arises from accommodating three, essentially, co-planar pyridyl groups at the metal center [pyridyl groups have twist angles of 13.6(1), 17.3(1)

and 36.2(1) o out of the AgN3 coordination plane]. The metal ion lies slightly out of the mean plane of the coordinating atoms, by 0.22(1) Å, which are bonded in a distorted trigonal geometry (N1-Ag(1)-N1' = 122.16(1)o; N1'-Ag-N3 = 111.54(1)o; N1-Ag-N3 123.65(1)o Σ=357.35o). Two independent L1 ligands show anti-syn-anti and anti-anti-anti conformations. A pair of a-s-a-L1 coordinate Ag(I) ions to form a binuclear 30-membered Ag2L12 metallacyclic ring, which is linked into chains through the a-a-a-L1 conformer. The BF4- anions lie above and below the plane of the macrocyclic rings. The Ag…Ag distance across the macrocycle is 16.372(1) Å and between adjacent rings 17.931(1) Å. This type of metallacycle chain motif, though not without precedence,[6] is rather less common than other one-dimensional coordination topologies.

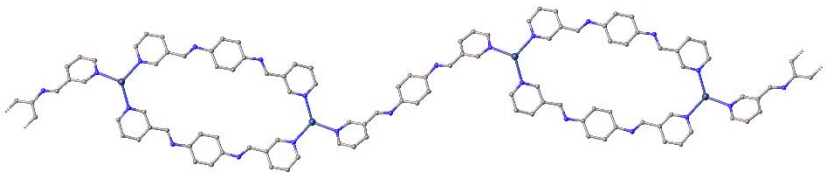

Figure 6. Molecular structure of 5 illustrating a cationic chain of ligand-bridged metallamacrocycles in the coordination polymer. The non-coordinated anion is omitted for clarity.

{[Ag(L2)]TFM}n 6

In an attempt to disentangle aromatic stacking and argentophilic effects, as reported for L1 in 1a,[20] we designed L2. This ligand features aromatic rings but, due to the bulky methyl groups, lacks □□□ stacking ability. Compound 6 crystallized in the monoclinic space group I2/a, and the asymmetric unit is constituted by one equivalent each of Ag(I), L2 and non-coordinating TFM anion. This 1:1 Ag:ligand stoichiometric compound features a cationic polymer chain based on distorted linear geometry at the metal center (Figure 7). The polymer chain is generated by inversion and is propagated in the [102] direction. The Ag(I) ion is coordinated by two crystallographically unique pyridyl N-atoms. The coordination environment has bond lengths Ag1-N1 2.154(3) and Ag1-N3 2.141(3) Å with a bond angle N1-Ag-N3 of 175.4(1)o. The TFM anion is disordered over two positions and is oriented with oxygen atoms directed towards Ag(I) ions, but at long range (Ag…O >2.85 Å). The L2 group adopts an anti-syn-anti conformation with the Ag-NPy coordination vectors lying on the same side of the central group. This produces a "sine wave" motif, though this has a ligand-centered crest/trough arrangement as compared to the metallo-centric cases in 1b and 3. The intra-chain Ag…Ag separation is increased, to 21.53(1) Å, due to the larger size of the central biphenyl unit in L2.

Noteworthy, however, is the presence of Ag…Ag interactions similar to those seen in 1a.[20] In 6 this interaction is generated by a 2-fold rotation axis forming pairs of coordination chains with Ag…Ag distance of 3.245(1) Å (Figure 8). Given the inability of L2 to form □□□ stacking this demonstrates that argentophilic interactions do not require such support.[10]

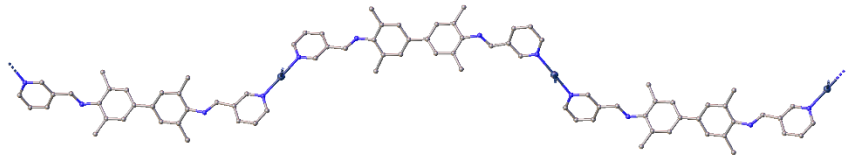

Figure 7. Molecular structure of a cationic coordination polymer chain in 6 highlighting "sine-wave" motif. The non-coordinated anion is omitted for clarity.

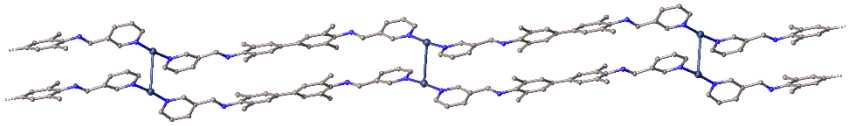

Figure 8. View of 6 highlighting the Ag…Ag pairing of adjacent chains. (H-atoms omitted for clarity).

{[Ag2(L3)(NO3)2]·2MeCN}n 7

In a further effort to explore the influence of ligand properties L3, with a cyclohexyl bridging unit, was prepared which substitutes the aromatic core in L1 with an aliphatic group of similar size. From the reaction of L3 with AgNO3 compound 7 was isolated which has a 1:1 Ag:ligand stoichiometry and which crystallized in the space group P $\bar{1}$. The asymmetric unit is constituted by one unit each of Ag(I), NO3-, MeCN and half an equivalent of L3. The one-dimensional polymer in this case has a tape motif (Figure 9). The silver ion adopts a distorted T-shape coordination geometry involving both imino and pyridyl N-donor atoms along with the oxygen of the NO3- anion. This O-atom lies 1.268(1) Å out of the AgN2 coordination plane. Bond lengths to the metal ion are; Ag-NImino 2.218(1), Ag-NPy, 2.255(1), Ag-O 2.500(1) Å. An MeCN solvent molecule is occluded in the crystal structure but is not involved in the coordination sphere (Ag…NMeCN 2.836(1) Å). The bound pyridyl group forms a coordination chain through translation along the [100] direction and the tape, generated by the imino interaction, forms across an inversion center. The ligand is located about an inversion center with anti-anti-anti conformation with the pyridyl N atoms directed in an opposing manner to one another, as well as to the nearest imino N-atom. The involvement of the imino N-atoms in the coordination generates dinuclear 22-membered Ag2L32 metallacyclic rings. These are fused into the resulting tape that has Ag…Ag separations of 8.025(1) Å down the tape axis and 7.780(1) Å across the tape width.

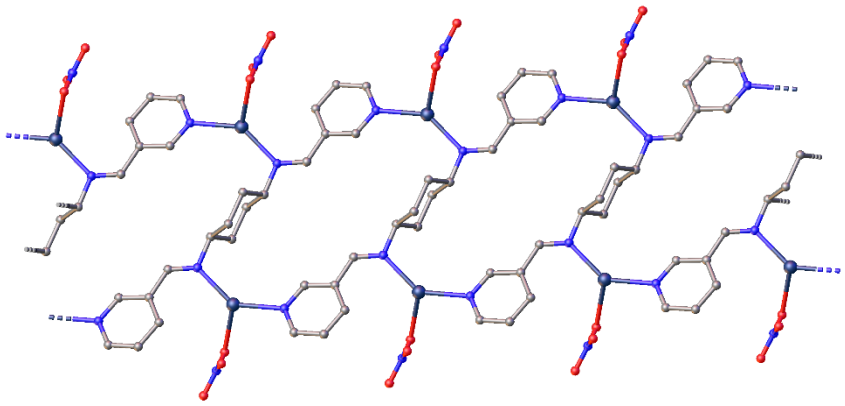

Figure 9. The molecular structure of 7 highlighting the 1D ribbon structure involving Ag-NPyridyl and Ag-NImino coordination which generate dinuclear 22-membered Ag2L32 metallacyclic rings.

{[Ag(L3)(Tos)]·½H2O}n 8

Reaction of L3 with Ag(Tos) gave 8 with a 1:1 Ag:ligand stoichiometry which crystallized in the space group P $\bar{1}$. The asymmetric unit contains two units each of Ag(I), L3 and tosylate anion as well as an occluded water molecule, all in general positions. The neutral coordination polymer is generated by inversion symmetry and is based on distorted T-shaped geometry involving NPyridyl and Otosylate coordination (Figure 10). There are only small differences in the nature of the independent metal ion sites. Bond lengths to the metal centers are Ag1-N1 2.149(1); Ag1-N8 2.146(1); Ag1-O1 2.555(1) and Ag2-N4 2.168(1) Ag2-N4 2.166(1) Å, Ag2-O4 2.509(1) Å). The metal-bound oxygen atoms lie significantly out of the associated AgN2 coordination planes by 1.088(1) and 0.703(1) Å for O1 and O4, respectively. Both L3 ligands adopt an anti-anti-anti conformation; however, these differ substantially with regard to the orientation of the N-C bonds to the central cyclohexyl group, with both axial (N6/N7) and equatorial (N2/N3) orientations being found. Individual polymer chains have L3 ligands with equatorial and axial orientations alternating along the length giving rise to slightly different intra-chain Ag…Ag separations, at 18.039(6) and 18.269(7) Å. The polymeric chain has a "saw-tooth" motif, as seen in 2 and 4, though this differs as each "tooth" contains [2Ag + 2L].

An interesting feature of 8 is the extended nature of the inter-metallic interactions (Figure 11). The crystal structure contains tetrameric groups of silver ions with Ag…Ag distances; Ag1…Ag1' 3.281(1) Å; Ag1…Ag2 3.217(1) Å; and with an Ag2-Ag1-Ag1' angle of 164.4o. These argentophilic interactions are unsupported by ligand bridging as in all the structures reported here. These tetramers are generated by inversion symmetry and are further related by inversion symmetry to adjacent tetramers at a longer distance of 3.583(1) Å. The resulting silver ion chains run throughout the crystal structure. Such extending stacking is seen in solid state structures of other Ag-coordination polymers, such as [Ag(en)]NO3 in which the Ag(I) ions are 2-coordinate.[24]

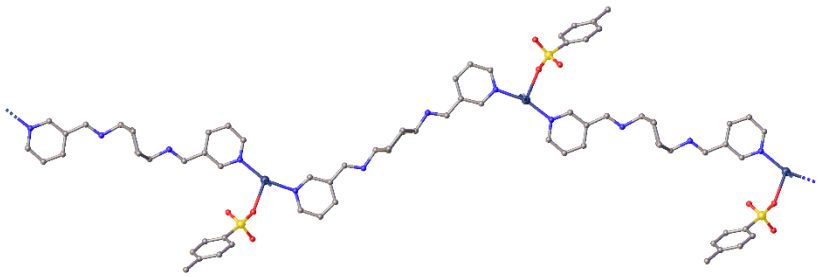

Figure 10. Molecular structure of 8 highlighting the [2Ag + 2L] "saw-tooth" motif of the coordination polymer chain. Ligands with axial or equatorial orientations alternate along the chain.

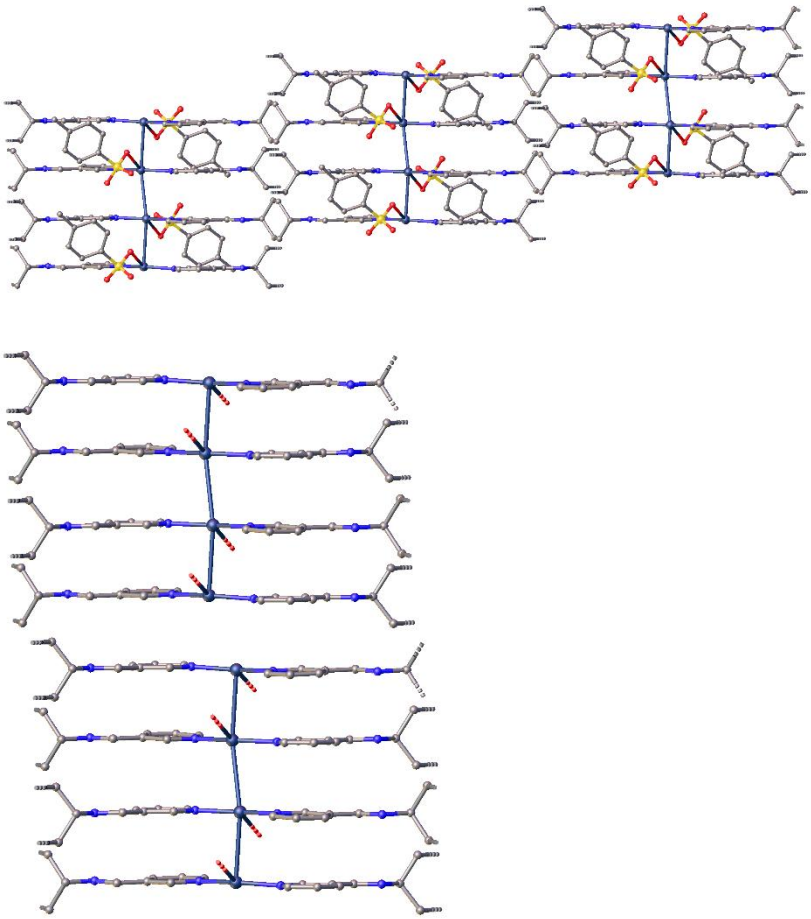

Figure 11. Inter-chain interactions in 8 are seen with (upper) tetrameric "stacks" formed by argentophilic interactions. Lower, continuous silver "chains" running through the crystal structure are formed by interactions between these tetrameric "stacks".

Despite repeated efforts, formation of 8 proved reproducibly elusive. However, from various attempts compounds 9 and 10 were also isolated.

{[Ag(L3)(Tos)]·DCM}n 9

Compound 9, a non-hydrate analogue of 8, was isolated and found to crystallize in the space group P $\bar{1}$. The asymmetric unit comprises one equivalent each of Ag(I), L3 and Tos- and all the atoms are in general positions. The structure forms a neutral one-dimensional chain polymer generated by inversion symmetry with a [1Ag + 1L] "saw tooth" motif (Figure 13). Similar to 8, the chain is based on a distorted T-shaped geometry with coordination of NPyridyl and Otosylate. Bond lengths to the metal center are; Ag1-N1 2.153(1); Ag1-N4 2.174(1); Ag1-O1 2.541(1) Å. The Ag(I) ion and coordinating atoms are essentially co-planar (maximum deviation ~0.12 Å). The L3 ligand adopts an anti-anti-anti conformation with equatorial arrangement of the pyridyl and cyclohexyl groups. As was generally found, the three rings of L3 are far from co-planar. Rather than the tetrameric silver units in 7, compound 8 features a pairwise interaction similar to 1a and 6, which is generated by inversion symmetry giving a Ag…Ag distance of 3.125(1) Å (Figure 14).

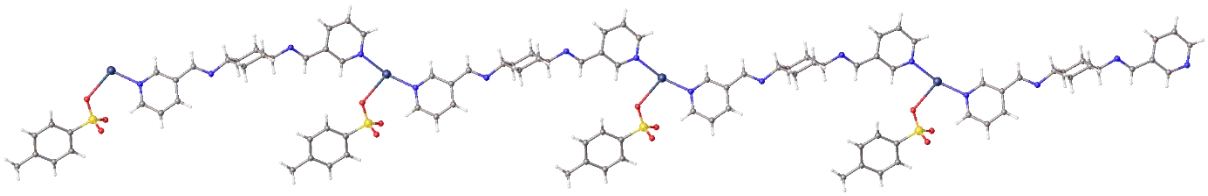

Figure 13. Molecular structure of 9 highlighting the neutral chain polymer with a [1Ag + 1L] "saw tooth" motif. Note the essentially orthogonal arrangement of the terminal pyridyl groups w.r.t. the central cyclohexyl group of L3.

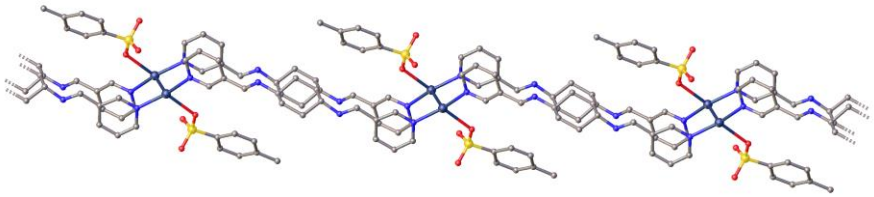

Figure 14. The pairwise interaction of adjacent polymer chains in 9 through Ag…Ag interactions involving the three-co-ordinate metal ions.

{[Ag(L3)0.5(Tos)]·4H2O}n 10

In a further attempt to reproduce 8 the crystallization process was modified by addition of water directly to the MeCN layer. While this also proved unsuccessful, it yielded 10. Compound 10 crystallized in the space group P $\bar{1}$ with the asymmetric unit comprising one unit each of Ag(I) and tosylate, half an equivalent of L3 and four molecules of water. The 2:1 Ag:ligand

stoichiometry of 10 features a metallacyclic chain structure, as in 5, though this bears no net charge due to anion coordination. The coordination of the unique Ag(I) ion comprises both imino and pyridyl N-donors and oxygen from the anion arranged in a distorted T-shaped geometry (Figure 15). Bond lengths are Ag-Npyridyl 2.230(1), Ag1-NImino 2.199(1), Ag1-O1 2.557(1). The dinuclear Ag2L32 metallacycles are substantially smaller, 12-membered rings, compared to those found in either 5 or 7. The smaller ring size arises from the syn-anti-syn ligand conformation in 10 which orients pyridyl and imino N-atoms on each unique half of the ligand in the same sense. The Ag…Ag distances are much shorter both within the metallacycle at 5.075(1) Å and between nearest neighbors along the chain viz. 7.971(1) Å.

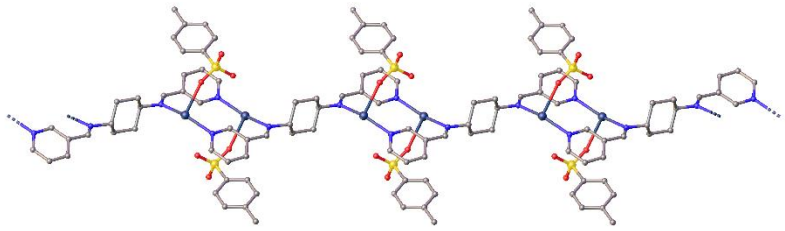

Figure 15. Molecular structure of 10 highlighting the 12-membered dinuclear Ag2L32 metallacyclic rings of the polymer chain.

The crystal structure includes four molecules of water in the asymmetric unit; these have a profound effect on arrangement of the metallacyclic chains. These are assembled into sheets through a network of three hydrogen-bonded rings. These involve two oxygen atoms of coordinated tosylate anion in addition to the water molecules (Figure 16). These sheets are stacked in the crystal structure through a second type of three-ringed hydrogen-bonded network comprising two hexacyclic {H2O}6 rings and a five-membered {(H2O)3(Tos)} ring involving tosylate oxygen atoms. Cyclic arrangements of water molecules can be also seen which form 4- and 6-membered rings, such as have been identified in liquid water (Figure 17).[25]

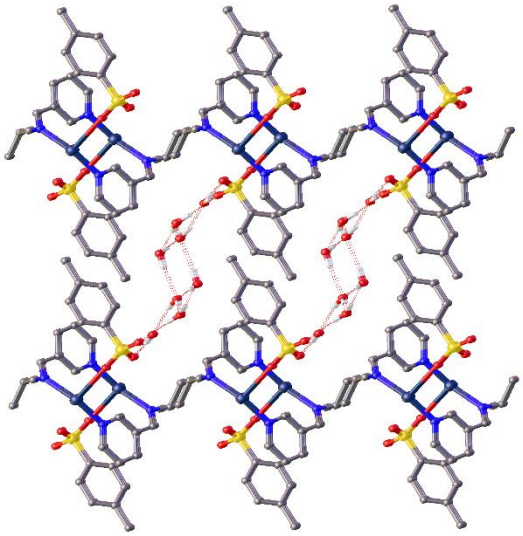

Figure 16. Individual metallacyclic chain polymers are linked into sheets through hydrogen-bonded tolsylate..{H2O}4…toslylate networks.

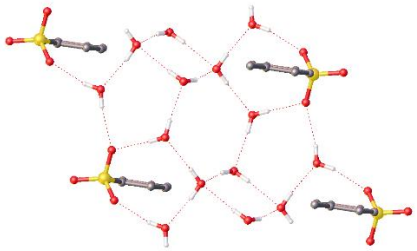

Figure 17. Water molecules in the crystal structure of 10 form four- and six-membered hydrogen-bonded cyclic structures as seen in liquid water.

Given the increased interest in argentophilicity[10] we examined those observed in the structure of compound 8 (Note: the sub-van der Waals distance for two Ag(I) ions is ca. 3.44 Å).[10] Mayer bond orders[26] (B.O.) were computed using DFT(PBEO) as implemented in the ORCA quantum chemistry package.[27] The bridging ligands were truncated as 2-methylpyridine groups. Calculations were performed for a single and a double tetrameric "stack" of complexes (see Figure 11), both with and without coordinated anions. Table 2 gives the values for bond order and the corresponding intermetallic distances.

Single stack (Ag4)	Distance/Å	Calculated Mayer B.O. (with anion)	Calculated Mayer B.O. (without anion)
Ag2…Ag1	3.22 Å	0.12	0.22
Ag1…Ag1'	3.28 Å	0.23	0.19

Table 2. Inter-metallic distances and calculated Mayer bond order for single four-silver "stack" structures.

For the single "stack" model with coordinated tosylate anion there is an approx. doubling of the bond order for the inner Ag1…Ag1' metal ions compared to the outer Ag2…Ag1 pairs (0.23 to 0.12). This is an unexpectedly large difference given the similarity in interatomic distance between the respective metal ions; in fact the higher bond order is for the slightly longer bond. In contrast, when the anions are removed the bond orders for the interactions become essentially equivalent at ~0.2%, as intuitively expected. A possible rationalisation for this can be found by examining the local environment of the metal ions pairs in the presence of the anions. The Ag2…Ag1 vector is in close proximity to hard oxygen atoms of the anionic tosylate group. In fact, the mid-point of the Ag2…Ag1 vector is closer to the coordinated oxygen atoms than the bond length to the bound metal atoms (O1…X = 2.1648(5) Å; O4…X = 2.1938(5) Å; where X = midpoint of the Ag…Ag vector; Ag1-O1 2.555(1); Ag2-O4 2.5009(1) Å). This electronically repulsive environment significantly reduces the metallophilic bonding between silver ions Ag2…Ag1. In contrast, the Ag1…Ag1 region is not influenced by anions in the same manner which, in turn, allows electron density to localise in the inter-metallic region giving a higher calculated bond order despite very similar distances. The local, non-bonded, environment has then a considerable effect on the metallophilic bonding.

Double stack (Ag8)	Distance/Å	Calculated Mayer B.O. (with anion)	Calculated Mayer B.O. (without anion)
Ag2…Ag1	3.22	0.12	0.22
Ag1…Ag1'	3.28	0.22	0.20
A1'…Ag2	3.22	0.14	0.22
Ag2…Ag2'	3.58	0.13	<0.1

Table 3. Inter-metallic distances and calculated Mayer bond order for double four-silver "stack".

By extending the model to include two tetrameric "stacks" this phenomenon is, again, observed. While the same trend is noted for the equivalent interactions, the presence of anions now enhances the metallophilic inter-stack interaction between Ag2…Ag2' to give a similar B.O. to Ag2…Ag1 (see Figure 11). This is despite the rather longer distance for the former. We are not aware of this phenomenon having previously been noted.

Conclusions

The new compounds described here extend the examples of one-dimensional Ag-containing coordination polymers and illustrate the suitability of (1-pyridin-3-yl)methanimines for generating a variety of structural types. These feature single chains, chains of metallocycles, and ribbon motifs. Within this series we have identified three new materials that feature argentophilic interactions, 6, 8 and 9 with Ag…Ag distances in the range 3.125 – 3.281 Å. These compounds variously highlight that (i) inter-metallic interactions do not require support from aromatic stacking and (ii) anion coordination is not necessary but can be tolerated. Both points are well illustrated by {[Ag(L2)]TFM}n 6.

Calculations indicate the sensitivity of intermetallic Ag…Ag interaction to the local environment – specifically, in this case, the influence of hard coordinated anions. The maximum bond order of ~20% could be reduced by almost 50% by the close proximity of anions. From an experimental viewpoint, the polymorph 1b, of the previously reported 1a, and a solvomorph 2 highlight that crystal packing forces and solvent inclusion can also readily disrupt these metallophilic interactions.

More generally, for silver coordination polymers product formation remains unpredictable with even poly- and solvo-morphic materials exhibiting differences in metal ion coordination geometry (compare 1a 1b and 2). Introducing modifications through ligand backbone and anion substitution obviously expands the variability further and, with this, the nature of the final solid-state form.

Experimental

General Conditions and Reagents. All reagents were purchased from Sigma-Aldrich or Alfa Aesar and used without further purification. FTIR spectra were recorded in air on a Shimadzu IRAffinity-1S. 1H NMR spectra were recorded on a Bruker AC300 spectrometer at 300 MHz in CDCl3 unless reported otherwise and referenced to residual non-deuterated solvent (δ 7.26). High-resolution electrospray (ESI) mass spectrometry (MS) spectra were recorded on a Waters Micromass LCT Premier TOF Mass Spectrometer.

Ligand synthesis. Ligands L1 and L3 were prepared by literature methods.[11], [22] For L2 procedure was as follows: 3,3′,5,5′-tetramethylbenzidine (6.0 g, 25 mmol) was dissolved in ethanol (50 ml) and dichloromethane (50 ml). Whilst stirring, nicotinaldehyde (5.36 g, 50 mmol) was added to the solution followed by two drops of formic acid. The solution was stirred at room temperature overnight. The sample was evaporated under reduced pressure until precipitation was observed. The solution was left to stand and vacuum assisted filtration followed by washing with ethanol (10 ml) and hexane (10 ml). (1E,1'E)-N,N'-(3,3',5,5'-tetramethyl-[1,1'-biphenyl]-4,4'-diyl)bis(1-(pyridin-3-yl)methanimine) (L2). Yellow crystalline powder (5.2 g 62 %). MP: 166-168 ˚C. FTIR: 1639 cm-1 s (imine CN). 1H NMR (CDCl3): δ 3.74 (12H, m), 7.35 (4H, s) 7.48 (2H, dd, J 7.9, 4.8), 8.35 (2H, s), 8.37 (2H dt, J 8.03, 1.91), 8.77 (2H, dd, J 4.8, 1.7), 9.05 (2H, d, J 1.5). Elemental analysis. Calc.(Found) C, 80.30(80.35); H, 6.29(6.26); N, 13.26(13.39). ESI-MS (M/z) 419.2230 (Calc. for M + H = 419.2236) Crystals of L2 were grown from CH2Cl2 and analysed by single crystal X-ray diffraction. Details are in the S.I.

Preparation of silver complexes 1-10. The general method for complex preparation was designed to yield single crystal samples using a liquid/liquid diffusion technique and not to optimize the synthetic method or yield. Briefly, L1, L2 or L3 was dissolved in dichloromethane (5 ml) and the desired silver salt dissolved in acetonitrile (5 ml) with the exception of 4 wherein the silver salt was dissolved in tetrahydrofuran (5 ml). Both solutions were cooled in card ice during and after the layering of the relevant solutions, the crystallisations were stored in the freezer (-20 ˚C), in a dark container for 3 days before transfer to a refrigerator for a further week. This method of reaction generally provided small numbers of single crystals suitable for analysis by X-ray diffraction. Reactions were typically performed for 1:1, 1:2 and 1:3 metal:ligand ratios, as it is known that reactions between Ag(I) ions and nitrogen donor ligands often show a lack of stoichiometric control and give heterogeneous products.[8, 21] For example with 5 a 2:3 ratio product was isolated from a 1:3 ratio reaction while 9 was a minor product isolated alongside the previously reported major product, {[Ag2(L3)(Tos)2]}n.[19] These issues precluded further analysis of bulk material in some cases.

Preparation of {[Ag(L1)NO3]}n (1b) and {[Ag(L1)]NO3•H2O}n (2). Silver nitrate (0.1 mmol, 17.0 mg) and L1 (0.1 mmol, 28.6 mg) were reacted using the previously described method and yellow single crystals suitable for X-ray analysis were obtained upon standing. Crystals of 2 and 1b were identified from the same 1:1 (M:L) stoichiometric reactions using single crystal X-ray diffraction. Crystals of 1b were also identified from 1:2 and 1:3 (M:L) stoichiometric reactions using single crystal X-ray diffraction. Decomposed: 225-227 ˚C. FTIR: 1613 cm-1 vs (imine C=N). This crystallization yielded a mixture of the products (identified by single crystal X-ray diffraction as 1a, 1b and 2) and satisfactory elemental analysis could not be obtained.

Preparation of {[Ag(L1)(TFA)]}n (3). Silver trifluoroacetate (0.1 mmol, 22.1 mg) and L1 (0.1 mmol, 28.6 mg) were reacted using the previously described method and yellow single crystals suitable for X-ray analysis were obtained upon standing. Crystals of 3 were also identified from 1:2 and 1:3 (M:L) stoichiometric reactions using single crystal X-ray diffraction. Decomposed: 210-212 ˚C. FTIR: 1622 cm-1 vs (imine C=N). Elemental analysis. Calc.(Found) C, 47.35(47.43); H, 2.79(2.78); N, 11.05(11.16).

Preparation of {[Ag(L1)]PF6}n (4). Silver hexafluorophosphate (0.1 mmol, 25.3 mg) and L1 (0.2 mmol, 57.2 mg) were reacted using the previously described method and yellow single crystals suitable for X-ray analysis were obtained upon standing, in addition to an amorphous powder. Elemental analysis suggested that 4 was a minor product in the reaction with the isolated material corresponding to an approx. 2:3 Ag:L1 stoichiometry.

Preparation of {[Ag(L1)1.5]BF4}n (5). Silver tetrafluoroborate (0.1 mmol, 19.5 mg) and L1 (0.3 mmol, 85.9 mg) were reacted using the previously described method and yellow single crystals suitable for X-ray analysis were obtained upon standing in addition to an amorphous powder. Crystals of 5 were also identified from 1:2 (M:L) stoichiometric reactions using single crystal X-ray diffraction. Decomposed: 226-228 ˚C. FTIR 1618 cm-1 vs (imine C=N). Elemental analysis. Calc.(Found) C, 51.95(51.76); H, 3.40(3.49); N, 13.47(13.40).

Preparation of {[Ag(L2)]TFM}n (6). Silver tetrafluoromethanesulfonate (0.1 mmol, 25.7 mg) and L2 (0.1 mmol, 41.9 mg) were reacted using the previously described method and yellow single

crystals suitable for X-ray analysis were obtained upon standing in addition to an amorphous material. Crystals of 6 were also identified from 1:2 and 1:3 (M:L) stoichiometric reactions using single crystal X-ray diffraction. Decomposed: 230-232 ˚C. FTIR: 1641 cm-1 vs (imine C=N). Elemental analysis. Calc.(Found) C, 51.57(49.6); H, 3.88(3.85); N, 8.29(7.86). Preparation of {[Ag2(L3)(NO3)2]·2MeCN}n (7). Silver nitrate (0.1 mmol, 17.0 mg) and L3 (0.1 mmol, 29.2 mg) were reacted using the previously described method and colourless single crystals suitable for X-ray analysis were obtained upon standing in addition to an amorphous material. Decomposed: 212-214 ˚C. FTIR: 1641 cm-1 vs (imine C=N). Further analysis could not be obtained due to the small quantity of material isolated.

Preparation of {[Ag(L3)(Tos)]·½H2O}n (8). Silver tosylate (0.1 mmol, 27.9 mg) and L3 (0.2 mmol, 58.5 mg) were reacted using the previously described method and a few colourless single crystals suitable for X-ray analysis were obtained upon standing. Decomposed: 230-232 ˚C. FTIR: 1638 cm-1 vs (imine C=N). Further analysis could not be obtained due to the small quantity of material isolated.

Preparation of {[Ag(L3)(Tos)]·DCM}n (9). Silver tosylate (0.1 mmol, 27.9 mg) and L3 (0.3 mmol, 87.7 mg) were reacted using the previously described method and colourless single crystals suitable for X-ray analysis were obtained upon standing. Decomposed: 234-235 ˚C. FTIR: 1638 cm-1 vs (imine C=N). It should be noted that we have previously characterized a 2D coordination polymer19 from these starting materials indicating the sensitivity of product formation to conditions. Elemental analysis of material isolated here was consistent with a 2:1 Ag:L3 stoichiometry indicating that 10 is a minor product in this reaction. Elemental analysis. Calc.(Found) C, 45.19(45.28); H, 4.03(4.16); N, 6.59(6.59).

Preparation of {[Ag(L3)0.5(Tos)]·4H2O}n (10). Silver tosylate (0.1 mmol, 27.9 mg), L3 (0.1 mmol, 29.2 mg) and H2O (1 ml) were reacted using the previously described method and colourless single crystals suitable for X-ray analysis were obtained upon standing. Decomposed: 198-199 ˚C. FTIR: 1643 cm-1 vs (imine C=N). Further analysis was not possible due to the small quantity of material isolated.

All crystal structure data, except those for 4 and 8, were collected on a Gemini A Ultra diffractometer equipped with an Oxford Cryosystems CryostreamPlus open-flow N2 cooling device. Data for 2, 3 and 9 were collected using molybdenum radiation (λMoKα = 0.71073 Å) and the intensities corrected for absorption using a multifaceted crystal model created by indexing the faces of the crystal for which data were collected.28 Data for 1, 5-7 and 10 were collected using copper radiation (λCuKα = 1.54184 Å) and the intensities corrected for absorption empirically using spherical harmonics. Data were collected at 150 K except in the case of 3 for which data were collected at 240 K as crystals of this compound underwent a phase transition at lower temperatures. Cell refinement, data collection and data reduction were undertaken via the software CrysAlisPro.29

Data for 4, 8 and L2 were collected at 100 K on beamline I19 at Diamond Light Source using synchrotron radiation (λ = 0.6889 Å) and the data processed using the software APEX2 [3].30 All structures were solved using SHELXT31 and refined by SHELXL32 using the Olex2 interface 6].33 All non-hydrogen atoms were refined anisotropically and hydrogen atoms were positioned

with idealised geometry, with the exception of those bound to heteroatoms, the positions of which were located using peaks in the Fourier difference map. The displacement parameters of the hydrogen atoms were constrained using a riding model with U(H) set to be an appropriate multiple of the Ueq value of the parent atom. The structure of 6 contains solvent-accessible voids that appear to hold multiple orientations of partially-occupied dichloromethane molecules. No sensible model could be applied to this disordered solvent, hence the electron density within the voids was treated using the Olex2 solvent mask routine.

References

1. Chen, C.-T.; Suslick, K. S., One-dimensional coordination polymers: Applications to material science. Coord. Chem. Rev. 1993, 128, 293-322.

2. Robin, A. Y.; Fromm, K. M., Coordination polymer networks with O- and N-donors: What they are, why and how they are made. Coord. Chem. Rev. 2006, 250, 2127–2157.

3. Givaja, G.; Amo-Ochoa, P.; Gómez-García, C. J.; Zamora, F., Electrical conductive coordination Polymers. Chem. Soc. Rev. 2012, 41, 115-147.

4. Khlobystov, A. N.; Blake, A. J.; Champness, N. R.; Lemenovskii, D. A.; Majouga, A. G.; Zyk, N. K.; Schroder, M., Supramolecular design of one-dimensional coordination polymers based on silver(I) complexes of aromatic nitrogen-donor ligands. Coord. Chem. Rev. 2001, 222, 155–192.

5. Munakata, M.; Wu, L. P.; Kuroda-Sowa, T., Silver(l) coordination complexes of 1,10-Phenanthroline-5,6-dione with 1D chain and 2D network structure. Adv. Inorg. Chem. 1999, 46, 173-303.

6. Oxtoby, N. S.; Blake, A. J.; Champness, N. R.; Wilson, C., Using multimodal ligands to influence network topology in silver(I) coordination polymers. PNAS 2002, 99, 4905–4910.

7. Steel, P. J.; Fitchett, C. M., Metallosupramolecular silver(I) assemblies based on pyrazine and related ligands. Coord. Chem. Rev. 2008, 252, 990–1006.

8. Zheng, S.-L.; Tong, M.-L.; Chen, X.-M., Silver(I)-hexamethylenetetramine molecular architectures: from self-assembly to designed assembly. Coord. Chem. Rev. 2003, 246, 185–202.

9. Young, A. G.; Hanton, L. R., Square planar silver(I) complexes: A rare but increasingly observed stereochemistry for silver(I). Coord. Chem. Rev. 2008, 252, 1346-1386.

10. Schmidbaur, H.; Schier, A., Argentophilic Interactions. Andew. Chem. Int. Ed. 2015, 54, 746-784.

11. Dong, Y. B.; Xu, H. X.; Ma, J. P.; Huang, R. O., Silver(I) coordination polymers based on a nano-sized bent bis(3-acetylenylphenyl-(4-cyanophenyl))oxadiazole ligand: The role of ligand

isomerism and the templating effect of polyatomic anions and solvent intermediates. Inorg. Chem. 2006, 45, 3325-3343.

12. Jin, F.; Zhang, Y.; Wang, H. Z.; Zhu, H. Z.; Yan, Y.; Zhang, J.; Wu, J. Y.; Tian, Y. P.; Zhou, H. P., Diverse Structural Ag(I) Supramolecular Complexes Constructed from Multidentate Dicyanoisophorone-Based Ligands: Structures and Enhanced Luminescence Cryst.Growth Des. 2013, 13, 1978-1987.

13. Genuis, E. D.; Kelly, J. A.; Patel, M.; McDonald, R.; Ferguson, M. J.; Greidanus-Strom, G., Coordination polymers from the self-assembly of silver(I) salts and two nonlinear aliphatic dinitrile ligands, cis-1,3-cyclopentanedicarbonitrile and cis-1,3-bis(cyanomethyl)cyclopentane: Synthesis, structures, and photoluminescent properties Inorg. Chem. 2008, 47, 6184-6194.

14. Bisht, K. K.; Kathalikkattilab, A. C.; Suresh, E., Structure modulation, argentophilic interactions and photoluminescence properties of silver(I) coordination polymers with isomeric N-donor ligands RSC Advances 2012, 2, 8421-8428.

15. Jin, X.; Tan, X. J.; Zhang, X. M.; Han, M. Y.; Zhao, Y. X., In vitro and in vivo anticancer effects of singly protonated dehydronorcantharidin silver coordination polymer in CT-26 murine colon carcinoma model. Bioorg. Med. Chem. Lett. 2015, 25, 4477-4480.

16. Fromm, K. M., Silver coordination compounds with antimicrobial properties Appl. Organomet. Chem. 2013 27, 683-687.

17. Cardoso, J. M. S.; Galvao, A. M.; Guerreiro, S. I.; Leitao, J. H.; Suarez, A. C.; Carvalho, M. F. N. N., Antibacterial activity of silver camphorimine coordination polymers. Dalton Trans. 2016, 45, 7114-7123.

18. Fei, H.; Rogow, D. L.; Oliver, S. R. J., Reversible Anion Exchange and Catalytic Properties of Two Cationic Metal-Organic Frameworks Based on Cu(I) and Ag(I). J. Am. Chem. Soc. 2010, 132, 7202-7209.

19. Lamming, G.; El-Zubir, O.; Kolokotroni, J.; McGurk, C.; Waddell, P.; Probert, M.; Houlton, A., Two-Dimensional frameworks based of Ag(I)-N bond formation: Single crystal to single molecular sheet transformation. Inorg. Chem. 2016, 55, 9644–9652.

20. Liu, Y.-H.; Xu, Q.; Han, Z.-Y., catena-((mu2-N,N'-bis(3-pyridylmethylidene)benzene-1,4-diamine)-(nitrato)-silver(i)). Acta Crystallogr.,Sect.E:Struct.Rep.Online 2010, 66, m903.

21. Blake, A. J.; Champness, N. R.; Cooke, P. A.; Nicolson, J. E. B.; Wilson, C., Multi-modal bridging ligands; effects of ligand functionality, anion and crystallisation solvent in silver(I) co-ordination polymers. J. C. S. Dalton Trans. 2000, 3811–3819.

22. Kim, H. N.; Lee, H. K.; Lee, S. W., N,N'-bis(3-Pyridylmethylene)-p-phenylenediamine P21 155-157 deg.C ACICAR. Bull. Korean Chem. Soc. 2005, 26, 892.

23. Ha, K., A centrosymmetric monoclinic polymorph of N,N-bis-(pyridin-3-yl-methyl-idene)benzene-1,4-diamine. Acta Crystallogr Sect E Struct Rep Online. 2011, 67, o2250.

24. Cai, W.; Katrusiak, A., Giant negative linear compression positively coupled to massive thermal expansionin a metal–organic framework. Nature Commun. 2014, 5, 4337.

25. Ludwig, R., Water: From clusters to the bulk Angew. Chem. Int. Ed. 2001, 40, 1808-1827.

26. Mater, I., Charge, bond order and valence in the AB initio SCF theory. Chem. Phys. Lett. 1983, 97, 270-274.

27. Neese, F., The ORCA program system. Wiley Interdiscipl. Rev. Comput. Mol. Sci. 2011, 2, 73-78.

28. Clark, R. C.; Reid, J. S., OLEX2. Acta Cryst. 1995, A51, 887-897.

29. CrysAlisPro Rigaku Oxford Diffraction,, Tokyo, Japan.

30. APEX2 Bruker AXS inc., Madison, Wisconsin,USA.

31. Sheldrick, G. M., SHELX XT. Acta Cryst. 2015, A71, 3-8.

32. Sheldrick, G. M., SHELX XL. Acta Cryst. 2008, A64, 112-122.

33. Dolomanov, O. V.; Bourhis, L. J.; Gildea, R. J.; Howard, J. A. K.; Puschmann, H., OLEX2: a complete structure solution, refinement and analysis program. J. Appl. Cryst 2009, 42, 339-341.

ASSOCIATED CONTENT

Supporting Information. This material (X-ray Crystallographic information (CIF)) is available free of charge via the Internet at http://pubs.acs.org.

AUTHOR INFORMATION

Corresponding Author

*Prof. Andrew Houlton, Chemical Nanoscience Lab, School of Chemistry, Newcastle University, Newcastle upon Tyne, NE17RU.

ACKNOWLEDGMENT

This work was supported in part by the School of Chemistry, Newcastle University and Akzo Nobel (G.L) and the EPSRC (EP/K018051/1). The authors thank Diamond Light Source for access to beamline I19.

For Table of Contents Use Only

Structural Diversity and Argentophilic Interactions in 1-D Silver-based Coordination Polymers

Glenn Lamming, James Kolokotroni, Thomas Harrison, Thomas J. Penfold, William Clegg, Paul G. Waddell, Michael R. Probert, Andrew Houlton

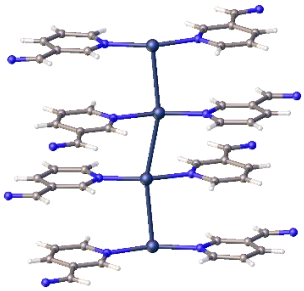

Employment of poly-monodentate ligands based on (1E,1'E')-N,N'-(-bis(1-pyridin-3-yl)methanimine with Ag(I) ions yield 1D coordination polymers with a range of single chain, metallacyclic and tape based motifs that can feature extended Ag…Ag interactions.

Structural Diversity and Argentophilic Interactions in 1-D Silver-based Coordination Polymers

Glenn Lamming, James Kolokotroni, Thomas Harrison, Thomas J. Penfold, William Clegg, ♯ Paul G. Waddell,♯ Michael R. Probert,♯ Andrew Houlton*
Chemical Nanoscience Laboratory, School of Chemistry, Newcastle University, Newcastle upon Tyne, NE1 7RU. ♯Crystallography Laboratory, School of Chemistry, Newcastle University, Newcastle upon Tyne, NE1 7RU

Single Crystal X-Ray Diffraction

{[Ag(L1)NO3]}n (1b)	
Empirical formula	C18H14AgN5O3
Formula weight	456.21
Temperature/K	150.0(2)
Crystal system	monoclinic
Space group	P21/n
a/Å	5.1579(2)
b/Å	15.9682(9)
c/Å	21.0358(9)
α/°	90
β/°	91.182(5)
γ/°	90
Volume/Å3	1732.19(14)
Z	4
ρcalcg/cm3	1.749
μ/mm-1	9.607
F(000)	912.0
Crystal size/mm3	0.29 × 0.12 × 0.04
Radiation	CuKα (λ = 1.54184)
2Θ range for data collection/°	6.95 to 132.648
Index ranges	-6 ≤ h ≤ 4, -16 ≤ k ≤ 18, -22 ≤ l ≤ 24
Reflections collected	7037
Independent reflections	2782 [Rint = 0.0478, Rsigma = 0.0526]
Data/restraints/parameters	2782/0/244
Goodness-of-fit on F2	1.066
Final R indexes [I>=2σ (I)]	R1 = 0.0498, wR2 = 0.1189
Final R indexes [all data]	R1 = 0.0684, wR2 = 0.1271
Largest diff. peak/hole / e Å-3	1.23/-0.58

Table S1: Crystal data and structure refinement for {[Ag(L1)NO3]}n (1b).

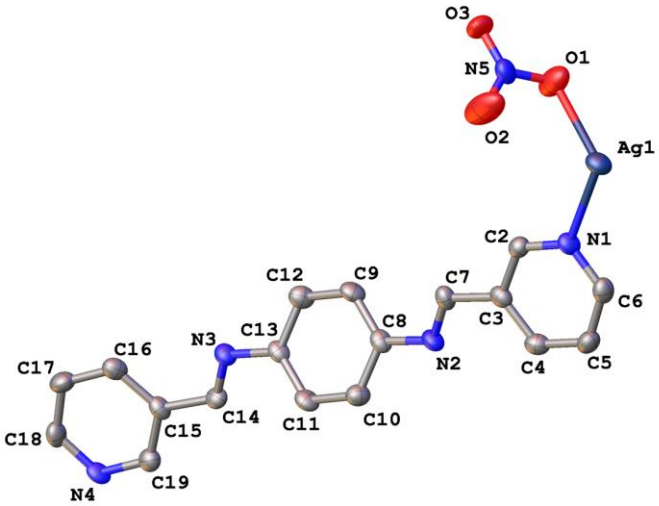

{[Ag(L1)]NO3·H2O}n (2)

Empirical formula	C18H16N5O4Ag
Formula weight	474.23
Temperature/K	150.01(10)
Crystal system	triclinic
Space group	P-1
a/Å	4.9087(4)
b/Å	8.8827(7)
c/Å	10.7282(10)
α/°	75.462(7)
β/°	84.917(7)
γ/°	76.056(7)
Volume/Å3	439.26(7)
Z	1
ρcalcg/cm3	1.793
μ/mm-1	1.185
F(000)	238.0
Crystal size/mm3	0.25 × 0.2 × 0.11
Radiation	MoKα (λ = 0.71073)
2Θ range for data collection/°	7.852 to 57.596
Index ranges	-6 ≤ h ≤ 6, -11 ≤ k ≤ 11, -14 ≤ l ≤ 14
Reflections collected	6999
Independent reflections	2011 [Rint = 0.0493, Rsigma = 0.0575]
Data/restraints/parameters	2011/107/151
Goodness-of-fit on F2	1.106
Final R indexes [I>=2σ (I)]	R1 = 0.0364, wR2 = 0.0613
Final R indexes [all data]	R1 = 0.0458, wR2 = 0.0656
Largest diff. peak/hole / e Å-3	0.41/-0.42

Table S2: Crystal data and structure refinement for {[Ag(L1)]NO3·H2O}n (2).

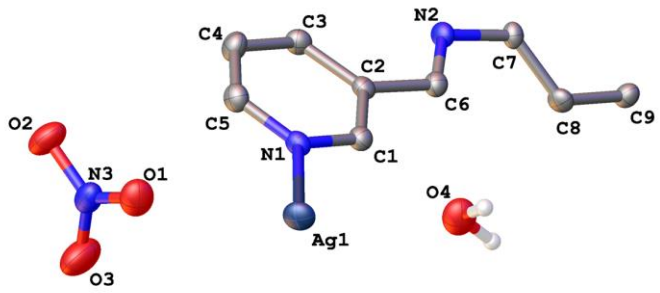

Figure S3. The asymmetric unit of the crystal structure of 2 with atomic displacement parameters (ADPs) drawn at the 50 % probability level. With the exception of those of the water molecule, hydrogen atoms have been omitted for clarity.

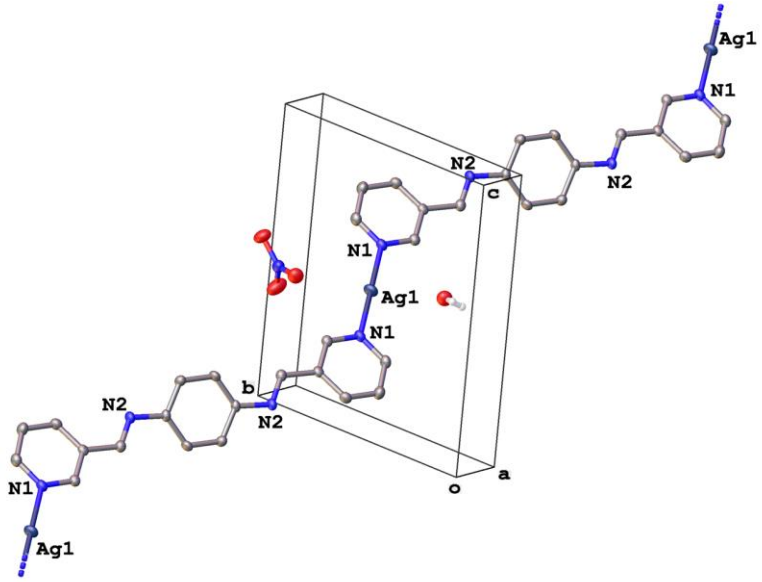

Figure S4. The structure of 2 illustrating the coordination about Ag1 with ADPs drawn at the 50% probability level. Hydrogen atoms and the labels for all hydrate, counterion and carbon atoms have been omitted for clarity.

{[Ag(L1)(TFA)]}n (3)

Empirical formula	C20H14AgF3N4O2
Formula weight	507.22
Temperature/K	240.0(2)
Crystal system	triclinic
Space group	P-1

a/Å	4.72483(13)
b/Å	9.5411(4)
c/Å	21.7160(9)
α/°	89.427(4)
β/°	87.768(3)
γ/°	75.667(3)
Volume/Å3	947.77(7)
Z	2
ρcalcg/cm3	1.777
μ/mm-1	1.118
F(000)	504.0
Crystal size/mm3	0.39 × 0.07 × 0.05
Radiation	MoKα (λ = 0.71073)
2Θ range for data collection/°	5.79 to 58.94
Index ranges	-6 ≤ h ≤ 6, -12 ≤ k ≤ 12, -28 ≤ l ≤ 29
Reflections collected	30130
Independent reflections	4537 [Rint = 0.0513, Rsigma = 0.0391]
Data/restraints/parameters	4537/117/289
Goodness-of-fit on F2	1.030
Final R indexes [I>=2σ (I)]	R1 = 0.0480, wR2 = 0.1086
Final R indexes [all data]	R1 = 0.0753, wR2 = 0.1218
Largest diff. peak/hole / e Å-3	0.58/-0.57

Table S3: Crystal data and structure refinement for {[Ag(L1)(TFA)]}n (3).

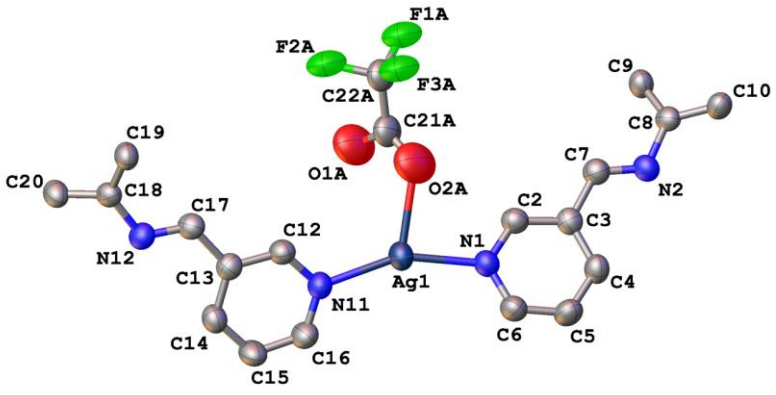

Figure S5. The asymmetric unit of the crystal structure of 3 with atomic displacement parameters drawn at the 50 % probability level. The triflate moiety was modelled as disordered over three positions and only the dominant orientation is depicted. Hydrogen atoms have been omitted for clarity.

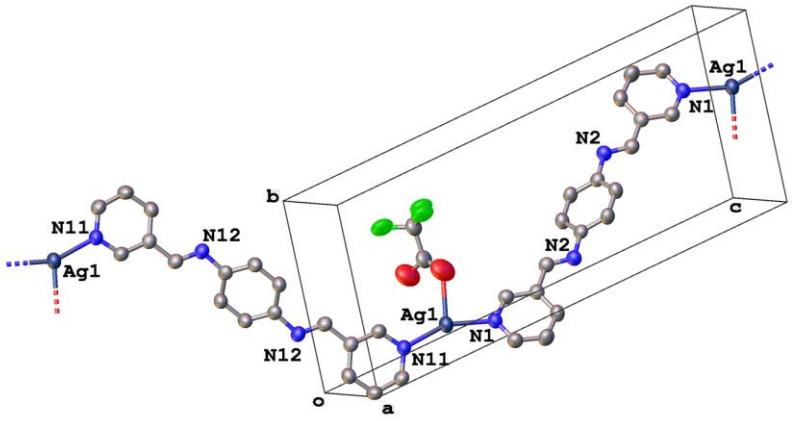

Figure S6. The structure of 3 illustrating the coordination about Ag1 with ADPs drawn at the 50% probability level. Hydrogen atoms and the labels for all but the nitrogen and silver atoms have been omitted for clarity.

{[Ag(L1)]PF6}n (4)	
Empirical formula	C18H14AgF6N4P
Formula weight	539.17
Temperature/K	100.0(2)
Crystal system	triclinic
Space group	P-1
a/Å	5.2090(7)
b/Å	8.4041(12)
c/Å	11.0852(15)
α/°	76.247(2)
β/°	89.323(3)
γ/°	75.087(3)
Volume/Å3	454.86(11)
Z	1
ρcalcg/cm3	1.968
μ/mm-1	1.179
F(000)	266.0
Crystal size/mm3	0.052 × 0.048 × 0.011
Radiation	Synchrotron (λ = 0.6899)
2Θ range for data collection/°	3.676 to 55.564
Index ranges	-7 ≤ h ≤ 7, -11 ≤ k ≤ 11, -14 ≤ l ≤ 14
Reflections collected	5624
Independent reflections	2311 [Rint = 0.0497, Rsigma = 0.0563]
Data/restraints/parameters	2311/0/139

Goodness-of-fit on F2	1.168
Final R indexes [I>=2σ (I)]	R1 = 0.0502, wR2 = 0.1384
Final R indexes [all data]	R1 = 0.0506, wR2 = 0.1388
Largest diff. peak/hole / e Å-3	3.62/-2.59

Table S4: Crystal data and structure refinement for {[Ag(L1)]PF6}n (4).

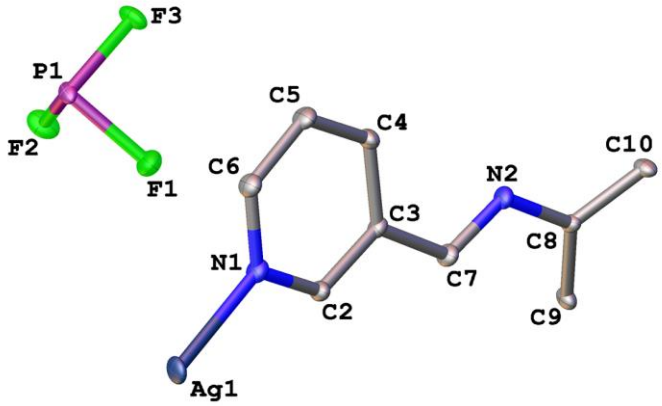

Figure S7. The asymmetric unit of the crystal structure of 4 with atomic displacement parameters drawn at the 50 % probability level. Hydrogen atoms have been omitted for clarity.

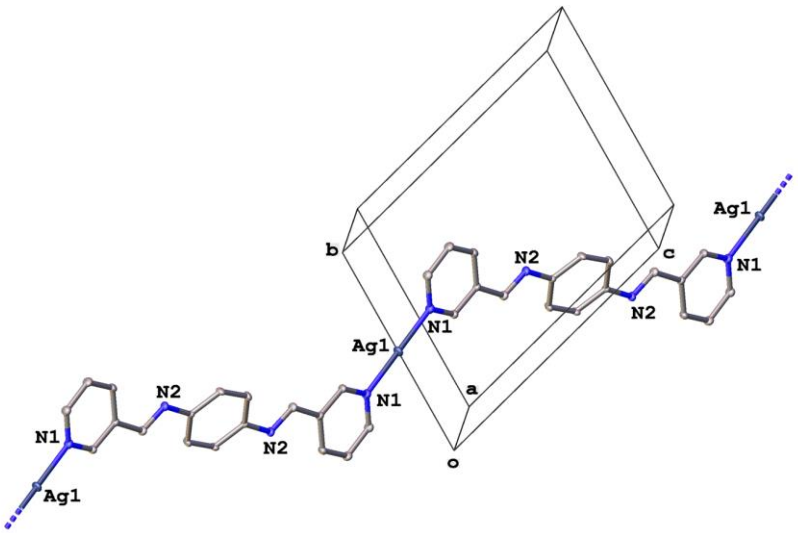

Figure S8. The structure of 4 illustrating the coordination about Ag1 with ADPs drawn at the 50% probability level. Hydrogen atoms, the hexafluorophosphate counterion and the labels for all but the nitrogen and silver atoms have been omitted for clarity.

{[Ag(L1)1.5]BF4}n (5)

Empirical formula	C27H21AgBF4N6

Formula weight	624.18
Temperature/K	150.0(2)
Crystal system	triclinic
Space group	P-1
a/Å	8.7101(3)
b/Å	10.2933(5)
c/Å	14.5291(7)
α/°	85.739(4)
β/°	79.546(4)
γ/°	72.930(4)
Volume/Å3	1224.26(10)
Z	2
ρcalcg/cm3	1.693
μ/mm-1	7.141
F(000)	626.0
Crystal size/mm3	0.19 × 0.05 × 0.03
Radiation	CuKα (λ = 1.54184)
2Θ range for data collection/°	6.188 to 133.956
Index ranges	-6 ≤ h ≤ 10, -12 ≤ k ≤ 12, -17 ≤ l ≤ 17
Reflections collected	17313
Independent reflections	4334 [Rint = 0.0685, Rsigma = 0.0535]
Data/restraints/parameters	4334/0/352
Goodness-of-fit on F2	1.036
Final R indexes [I>=2σ (I)]	R1 = 0.0337, wR2 = 0.0742
Final R indexes [all data]	R1 = 0.0456, wR2 = 0.0808
Largest diff. peak/hole / e Å-3	0.42/-0.51

Table S5: Crystal data and structure refinement for {[Ag(L1)1.5]BF4}n (5).

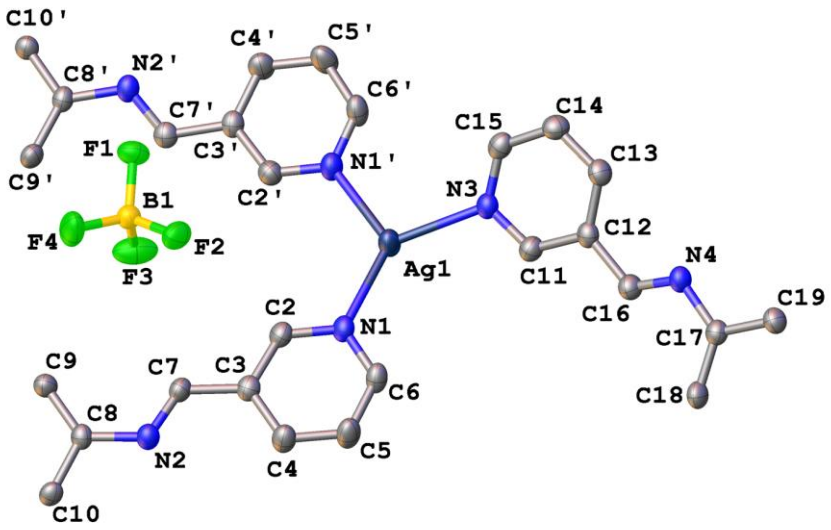

Figure S9. The asymmetric unit of the crystal structure of 5 with atomic displacement parameters drawn at the 50 % probability level. Hydrogen atoms have been omitted for clarity.

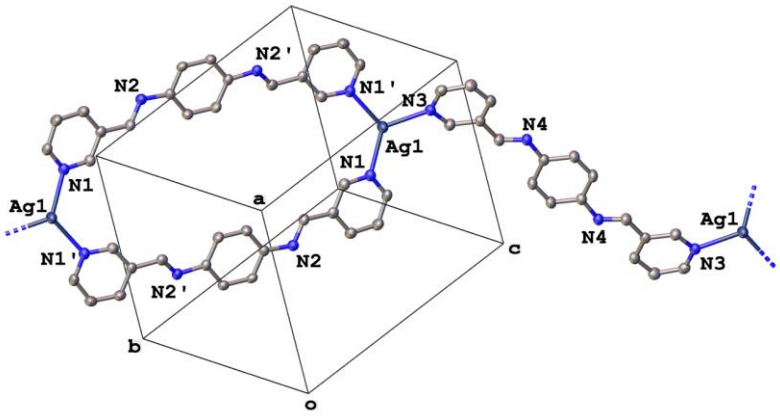

Figure S10. The structure of 5 illustrating the coordination about Ag1 with ADPs drawn at the 50% probability level. Hydrogen atoms, the tetrafluoroborate counterion and the labels for all but the nitrogen and silver atoms have been omitted for clarity.

{[Ag(L2)]TFM}n (6)	
Empirical formula	C29H26AgF3N4O3S
Formula weight	675.47
Temperature/K	150.0(2)
Crystal system	monoclinic
Space group	I2/a
a/Å	17.5883(3)
b/Å	10.51219(17)

c/Å	34.0537(5)
α/°	90
β/°	103.1271(14)
γ/°	90
Volume/Å3	6131.69(17)
Z	8
ρcalcg/cm3	1.463
μ/mm-1	6.379
F(000)	2736.0
Crystal size/mm3	0.26 × 0.14 × 0.11
Radiation	CuKα (λ = 1.54184)
2Θ range for data collection/°	5.33 to 133.788
Index ranges	-20 ≤ h ≤ 20, -11 ≤ k ≤ 12, -36 ≤ l ≤ 40
Reflections collected	43887
Independent reflections	5459 [Rint = 0.0416, Rsigma = 0.0209]
Data/restraints/parameters	5459/175/392
Goodness-of-fit on F2	1.070
Final R indexes [I>=2σ (I)]	R1 = 0.0389, wR2 = 0.1011
Final R indexes [all data]	R1 = 0.0454, wR2 = 0.1053
Largest diff. peak/hole / e Å-3	0.88/-0.94

Table S6: Crystal data and structure refinement for {[Ag(L2)]TFM}n (6).

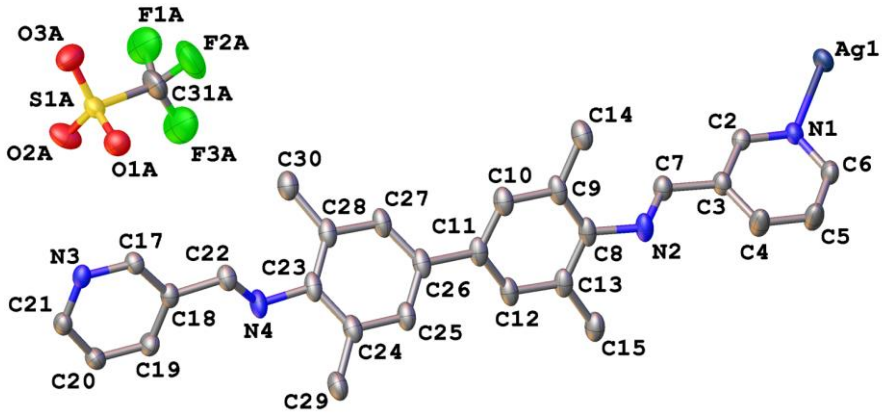

Figure S11. The asymmetric unit of the crystal structure of 6 with atomic displacement parameters drawn at the 50 % probability level. The triflouromethanesulfate moiety was modelled as disordered over two positions and only the dominant orientation is depicted. Hydrogen atoms have been omitted for clarity.

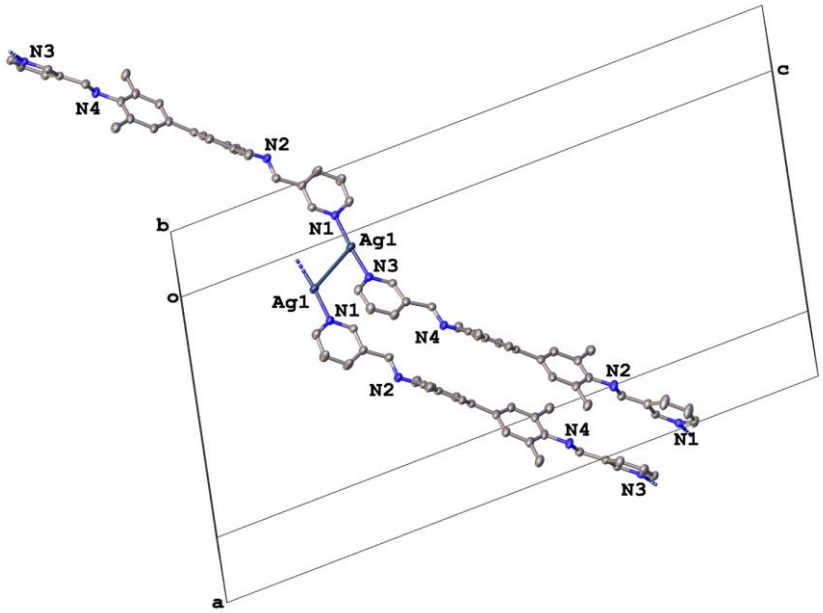

Figure S12. The structure of 6 illustrating the coordination about Ag1 with ADPs drawn at the 50% probability level. Hydrogen atoms and the labels for all but the nitrogen and silver atoms have been omitted for clarity.

{[Ag2(L3)(NO3)2]·2MeCN}n (7)

Empirical formula	C22H26N8O6Ag2
Formula weight	714.25
Temperature/K	150.0(2)
Crystal system	triclinic
Space group	P-1
a/Å	8.0247(3)
b/Å	8.1480(3)
c/Å	10.6157(4)
α/°	95.115(3)
β/°	95.458(3)
γ/°	109.856(4)
Volume/Å3	644.39(5)
Z	1
ρcalcg/cm3	1.841
μ/mm-1	12.663
F(000)	356.0
Crystal size/mm3	0.24 × 0.07 × 0.03
Radiation	CuKα (λ = 1.54184)
2Θ range for data collection/°	8.438 to 133.874
Index ranges	-9 ≤ h ≤ 9, -9 ≤ k ≤ 9, -12 ≤ l ≤ 12
Reflections collected	9173
Independent reflections	2279 [Rint = 0.0197, Rsigma = 0.0156]
Data/restraints/parameters	2279/0/173
Goodness-of-fit on F2	1.039

Final R indexes [I>=2σ (I)]	R1 = 0.0152, wR2 = 0.0381
Final R indexes [all data]	R1 = 0.0161, wR2 = 0.0385
Largest diff. peak/hole / e Å-3	0.25/-0.30

Table S7: Crystal data and structure refinement for {[Ag2(L3)(NO3)2]·2MeCN}n (7).

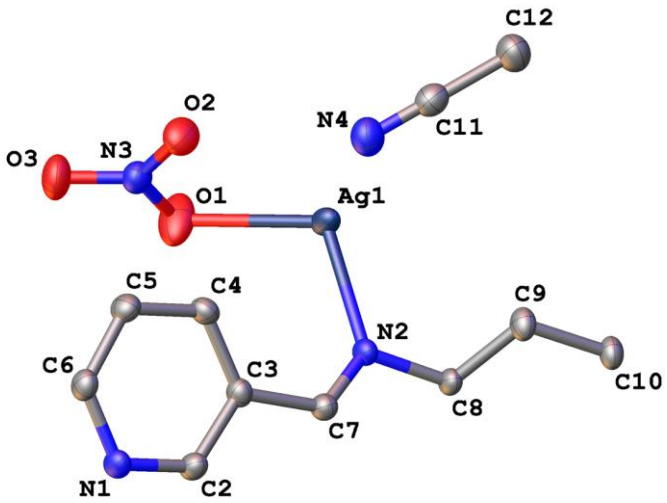

Figure S13. The asymmetric unit of the crystal structure of 7 with atomic displacement parameters drawn at the 50 % probability level. Hydrogen atoms have been omitted for clarity.

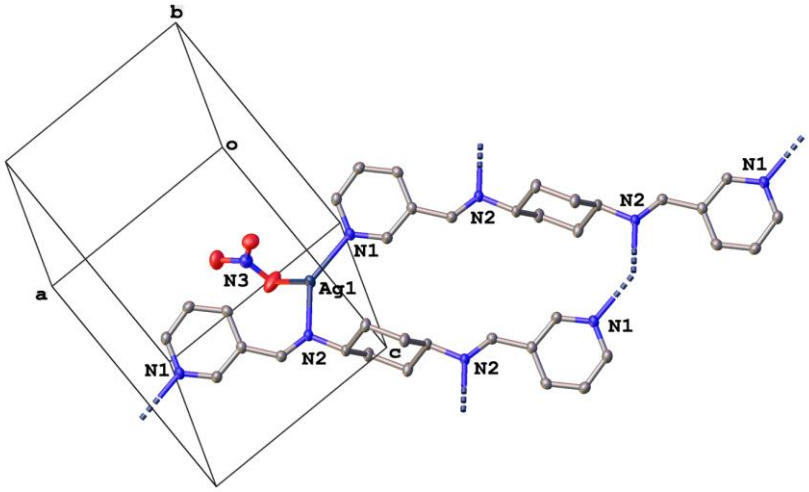

Figure S14. The structure of 7 illustrating the coordination about Ag1 with ADPs drawn at the 50% probability level. Hydrogen atoms and the labels for all but the nitrogen and silver atoms have been omitted for clarity.

{[Ag(L3)(Tos)]·½H2O}n (8)

Empirical formula	C25H28N4O3.5SAg
Formula weight	580.44

Temperature/K	100.15
Crystal system	triclinic
Space group	P-1
a/Å	12.586(4)
b/Å	12.603(4)
c/Å	18.483(7)
α/°	70.605(3)
β/°	86.715(5)
γ/°	62.368(3)
Volume/Å3	2433.6(14)
Z	4
ρcalcg/cm3	1.584
μ/mm-1	0.881
F(000)	1188.0
Crystal size/mm3	0.4 × 0.06 × 0.03
Radiation	synchrotron (λ = 0.6889)
2Θ range for data collection/°	3.564 to 53.334
Index ranges	-16 ≤ h ≤ 16, -16 ≤ k ≤ 16, -24 ≤ l ≤ 24
Reflections collected	18793
Independent reflections	18793 [Rint = 0.0150, Rsigma = 0.0501]
Data/restraints/parameters	18793/3/632
Goodness-of-fit on F2	0.987
Final R indexes [I>=2σ (I)]	R1 = 0.0332, wR2 = 0.0846
Final R indexes [all data]	R1 = 0.0387, wR2 = 0.0867
Largest diff. peak/hole / e Å-3	0.92/-1.05

Table S8: Crystal data and structure refinement for {[Ag(L3)(Tos)]·½H2O}n (8).

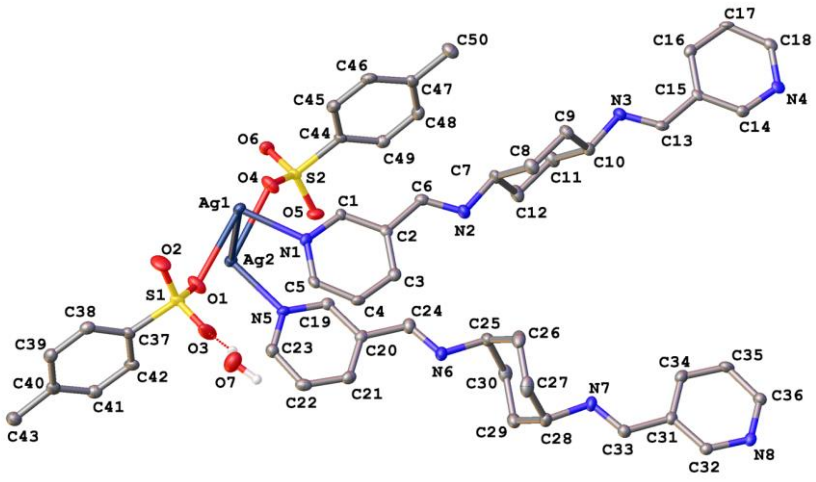

Figure S15. The asymmetric unit of the crystal structure of 8 with atomic displacement parameters

drawn at the 50 % probability level. With the exception of those of the water molecule, hydrogen atoms have been omitted for clarity. Dashed bonds denote hydrogen bonds.

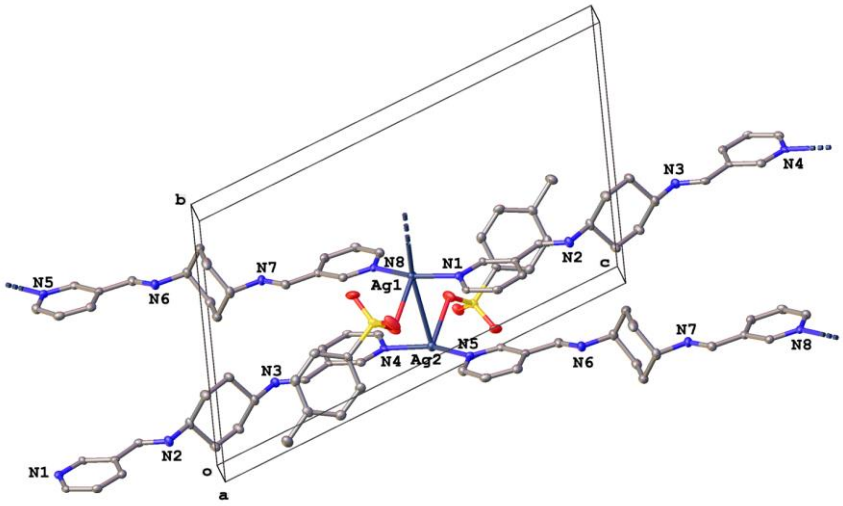

Figure S16. The structure of 8 illustrating the coordination about the two crystallographically independent silver atoms with ADPs drawn at the 50% probability level. Hydrogen atoms and the labels for all but the nitrogen and silver atoms have been omitted for clarity.

{[Ag(L3)(Tos)]·DCM}n (9)	
Empirical formula	C26H29AgCl2N4O3S
Formula weight	656.36
Temperature/K	150.0(2)
Crystal system	triclinic
Space group	P-1
a/Å	10.6683(7)
b/Å	11.3914(8)
c/Å	11.8059(7)
α/°	75.103(6)
β/°	75.633(6)
γ/°	81.974(6)
Volume/Å3	1338.75(16)
Z	2
ρcalcg/cm3	1.628
μ/mm-1	1.067
F(000)	668.0
Crystal size/mm3	0.2 × 0.09 × 0.08
Radiation	MoKα (λ = 0.71073)
2Θ range for data collection/°	5.788 to 57.82
Index ranges	-14 ≤ h ≤ 13, -15 ≤ k ≤ 15, -15 ≤ l ≤ 15
Reflections collected	22276

Independent reflections	6194 [Rint = 0.0476, Rsigma = 0.0551]
Data/restraints/parameters	6194/352/362
Goodness-of-fit on F2	1.062
Final R indexes [I>=2σ (I)]	R1 = 0.0508, wR2 = 0.1169
Final R indexes [all data]	R1 = 0.0754, wR2 = 0.1319
Largest diff. peak/hole / e Å-3	1.13/-1.29

Table S9: Crystal data and structure refinement for {[Ag(L3)(Tos)]·DCM}n (9).

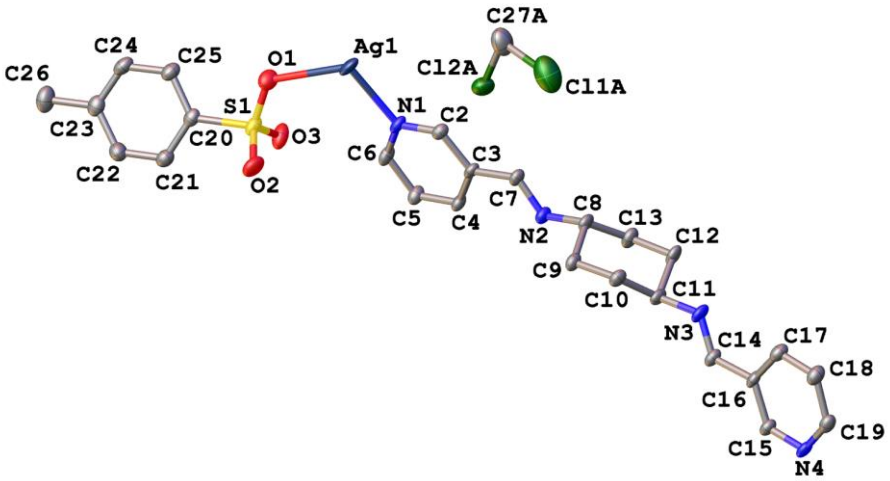

Figure S17. The asymmetric unit of the crystal structure of 9 with atomic displacement parameters drawn at the 50 % probability level. Hydrogen atoms have been omitted for clarity.

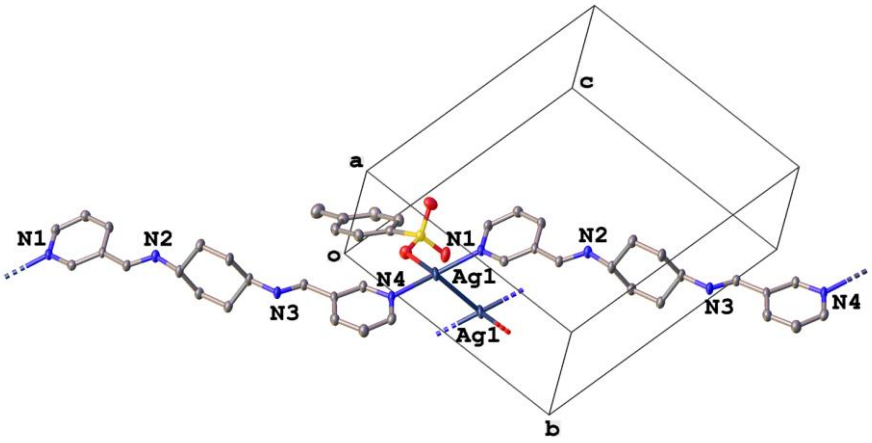

Figure S18. The structure of 9 illustrating the coordination about Ag1 with ADPs drawn at the 50% probability level. Hydrogen atoms and the labels for all but the nitrogen and silver atoms have been omitted for clarity.

{[Ag(L3)0.5(Tos)]·4H2O}n (10)

Empirical formula	C16H25AgN2O7S
Formula weight	497.31
Temperature/K	150.0(2)
Crystal system	triclinic
Space group	P-1
a/Å	7.3262(2)
b/Å	9.4198(3)
c/Å	14.2104(4)
α/°	89.965(2)
β/°	83.441(3)
γ/°	84.867(2)
Volume/Å3	970.31(5)
Z	2
ρcalcg/cm3	1.702
μ/mm-1	9.708
F(000)	508.0
Crystal size/mm3	0.37 × 0.25 × 0.17
Radiation	CuKα (λ = 1.54184)
2Θ range for data collection/°	6.262 to 133.854
Index ranges	-8 ≤ h ≤ 8, -10 ≤ k ≤ 11, -16 ≤ l ≤ 16
Reflections collected	16941
Independent reflections	3434 [Rint = 0.0529, Rsigma = 0.0311]
Data/restraints/parameters	3434/32/269
Goodness-of-fit on F2	1.063
Final R indexes [I>=2σ (I)]	R1 = 0.0266, wR2 = 0.0672
Final R indexes [all data]	R1 = 0.0273, wR2 = 0.0678
Largest diff. peak/hole / e Å-3	0.77/-0.83

Table S10: Crystal data and structure refinement for {[Ag(L3)0.5(Tos)]·4H2O}n (10).

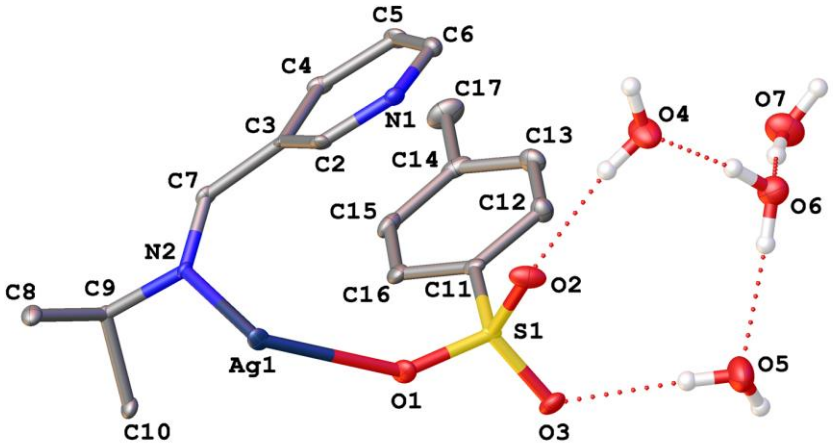

Figure S19. The asymmetric unit of the crystal structure of 10 with atomic displacement parameters drawn at the 50 % probability level. With the exception of those of the water molecules, hydrogen atoms have been omitted for clarity. Dashed lines denote hydrogen bonds.

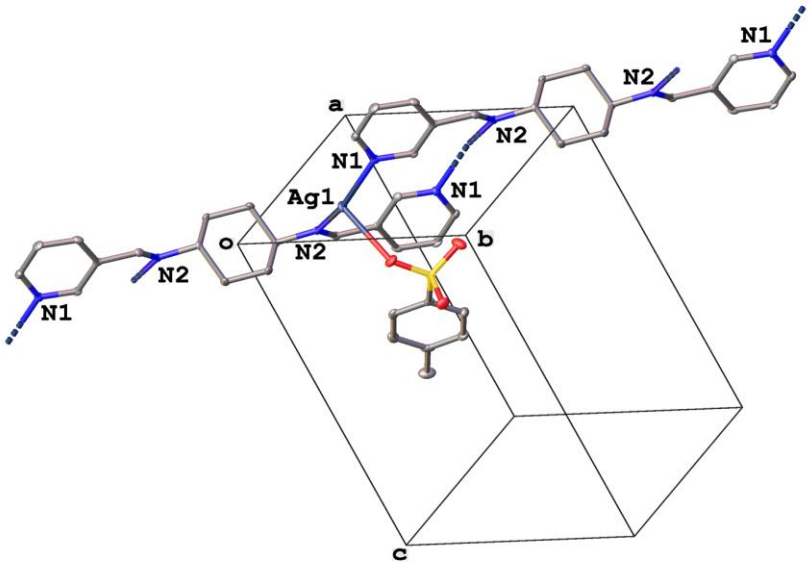

Figure S20. The structure of 10 illustrating the coordination about Ag1 with ADPs drawn at the 50% probability level. Hydrogen atoms and the labels for all but the nitrogen and silver atoms have been omitted for clarity.

L2

Empirical formula	C28H26N4
Formula weight	418.53
Temperature/K	100.0(2)
Crystal system	triclinic
Space group	P-1
a/Å	8.3080(7)
b/Å	8.5564(7)

c/Å	17.0592(14)
α/°	99.574(4)
β/°	96.649(4)
γ/°	107.159(4)
Volume/Å3	1124.94(16)
Z	2
ρcalcg/cm3	1.236
μ/mm-1	0.074
F(000)	444.0
Crystal size/mm3	0.11 × 0.1 × 0.01
Radiation	MoKα (λ = 0.71073)
2Θ range for data collection/°	2.458 to 50.054
Index ranges	-9 ≤ h ≤ 9, -10 ≤ k ≤ 10, -20 ≤ l ≤ 20
Reflections collected	8966
Independent reflections	3918 [Rint = 0.0461, Rsigma = 0.0894]
Data/restraints/parameters	3918/0/293
Goodness-of-fit on F2	1.031
Final R indexes [I>=2σ (I)]	R1 = 0.0496, wR2 = 0.1400
Final R indexes [all data]	R1 = 0.0662, wR2 = 0.1521
Largest diff. peak/hole / e Å-3	0.28/-0.26

Table S11: Crystal data and structure refinement for L2.

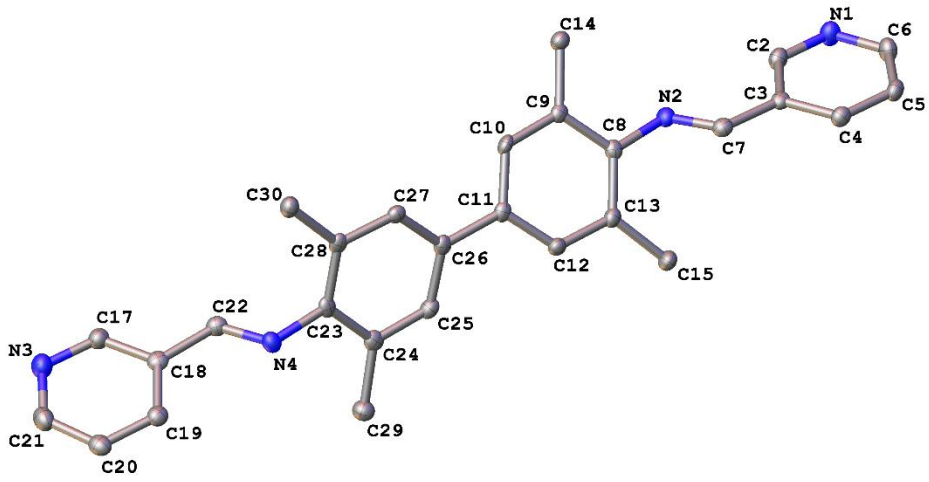

Figure S21. The asymmetric unit of the crystal structure of L2 with atomic displacement parameters drawn at the 50 % probability level. Hydrogen atoms have been omitted for clarity.